Extragalactic sources and propagation, including constraints on extragalactic magnetic fields

Arjen van Vliet
Rafael Alves Batista
Günter Sigl

UHECR2016

Universität Hamburg
DER FORSCHUNG | DER LEHRE | DER BILDUNG

CRPropa

Kyoto, Japan, 13/10/2016

Radboud University

Image: ASPERA

Measurements on UHECRs

SPECTRUM

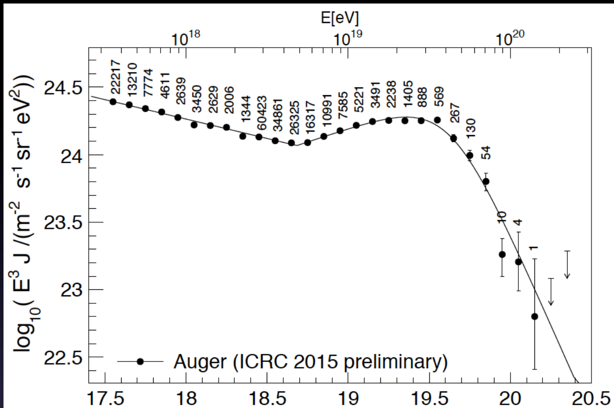

Auger, PoS (ICRC2015) 271

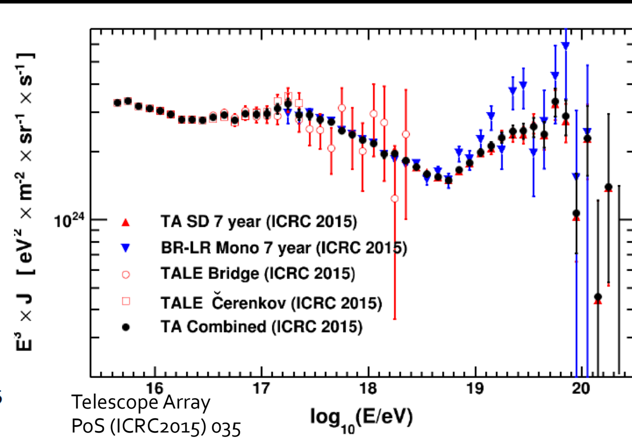

Telescope Array
PoS (ICRC2015) 035

ARRIVAL DIRECTION

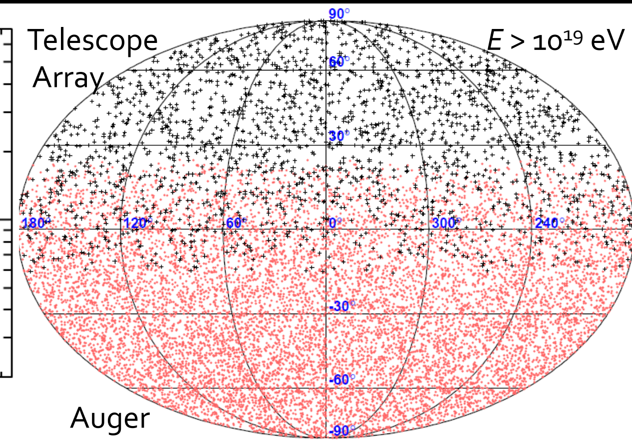

Telescope Array and Auger,
Astrophys. J. 794 (2014) 2, 172

COMPOSITION

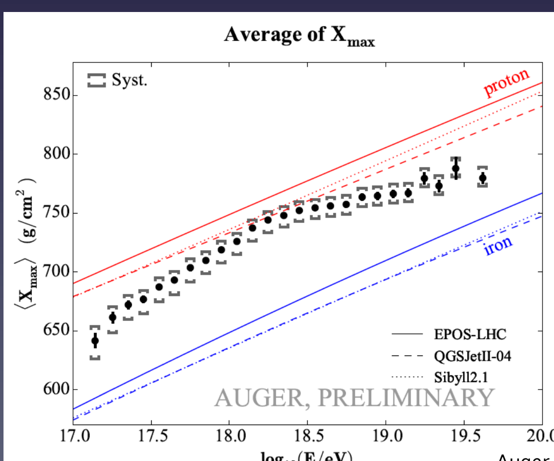

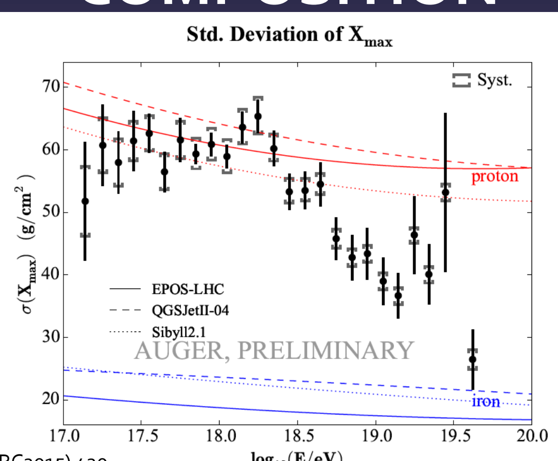

Auger, PoS (ICRC2015) 420

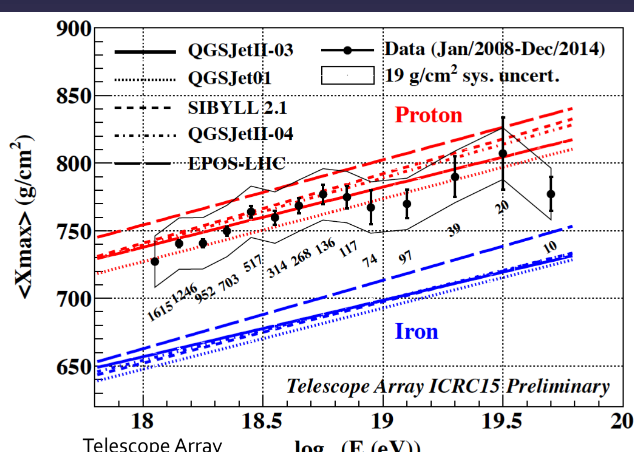

Telescope Array
PoS (ICRC2015) 320

UHECR secondaries

ASTROPHYSICAL NEUTRINO FLUX

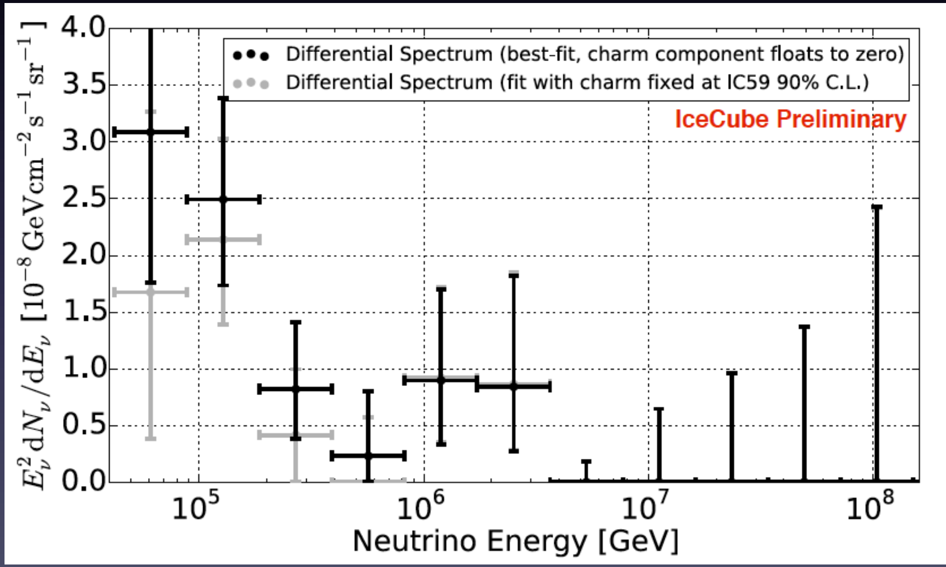

IceCube, PoS (ICRC2015) 1081

ISOTROPIC DIFFUSE γ-RAY BACKGROUND

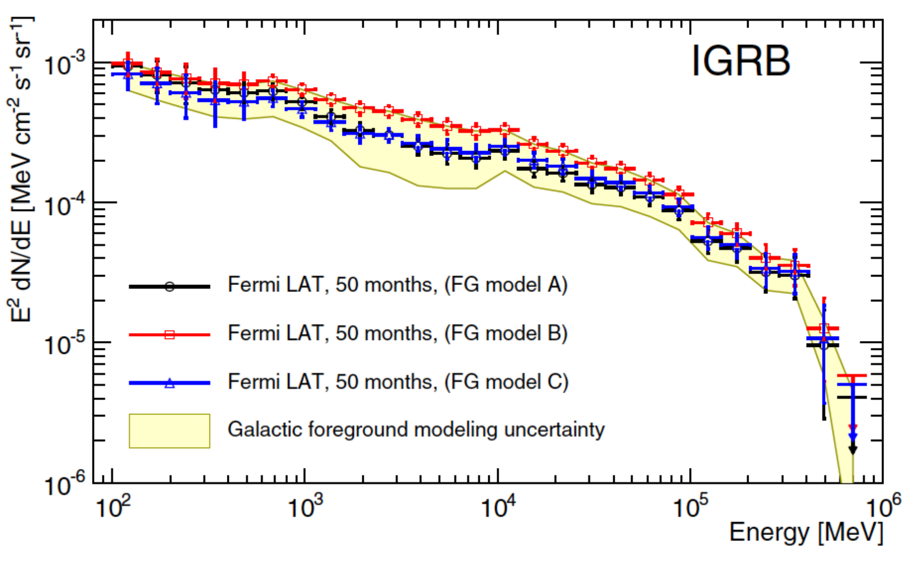

Fermi LAT, Astrophys. J. 799 (2015) 86

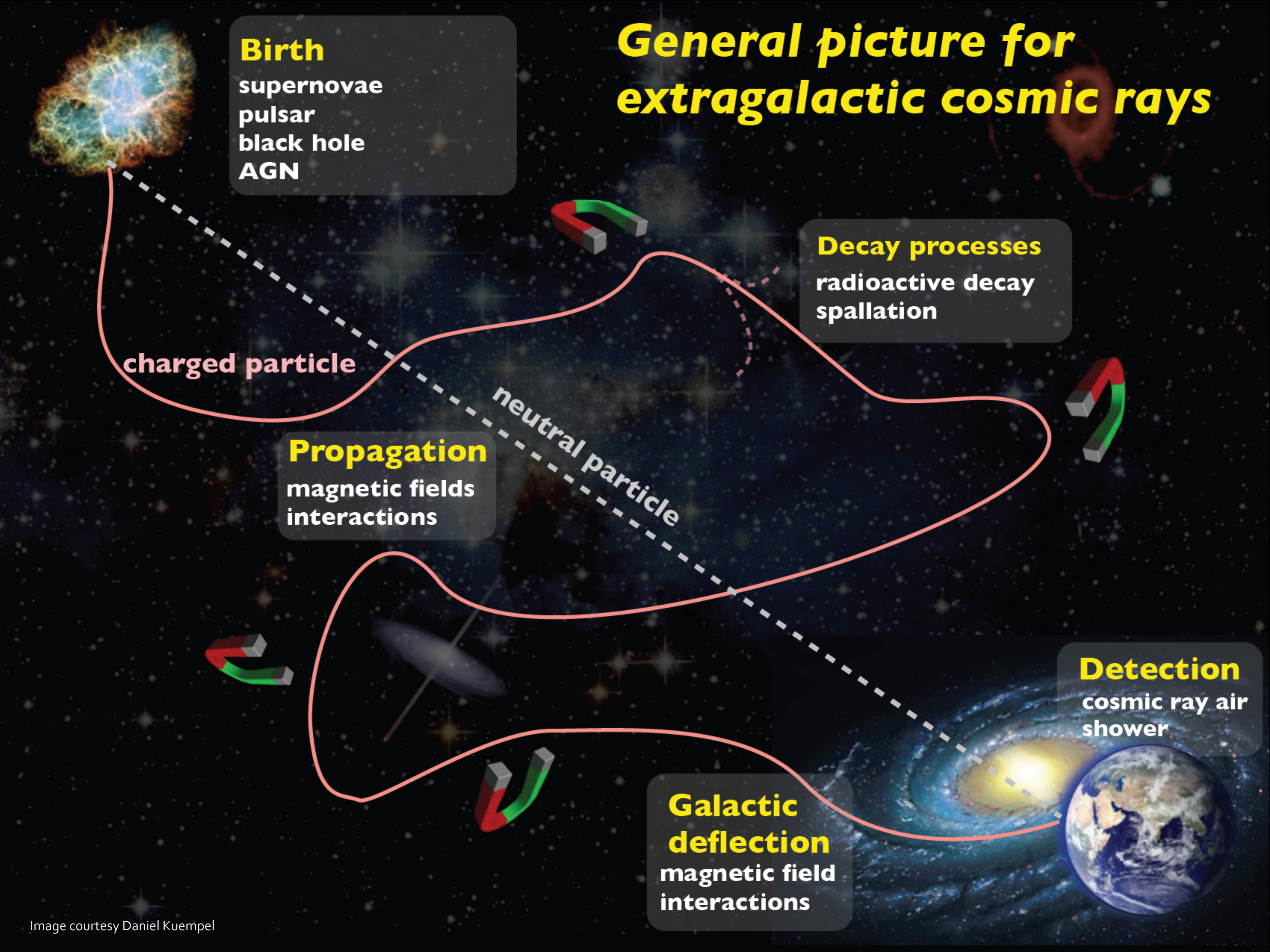
General picture for extragalactic cosmic rays
Birth
supernovae
pulsar
black hole
AGN
Decay processes
radioactive decay
spallation
charged particle
neutral particle
Propagation
magnetic fields
interactions
Detection
cosmic ray air shower
Galactic deflection
magnetic field
interactions
Image courtesy Daniel Kuempel

Extragalactic environment

- Source distribution following the Large-Scale Structure (LSS)
- Deflection in the extragalactic magnetic (EGMF)
- Example based on LSS formation simulations by Miniati et al. 2004:

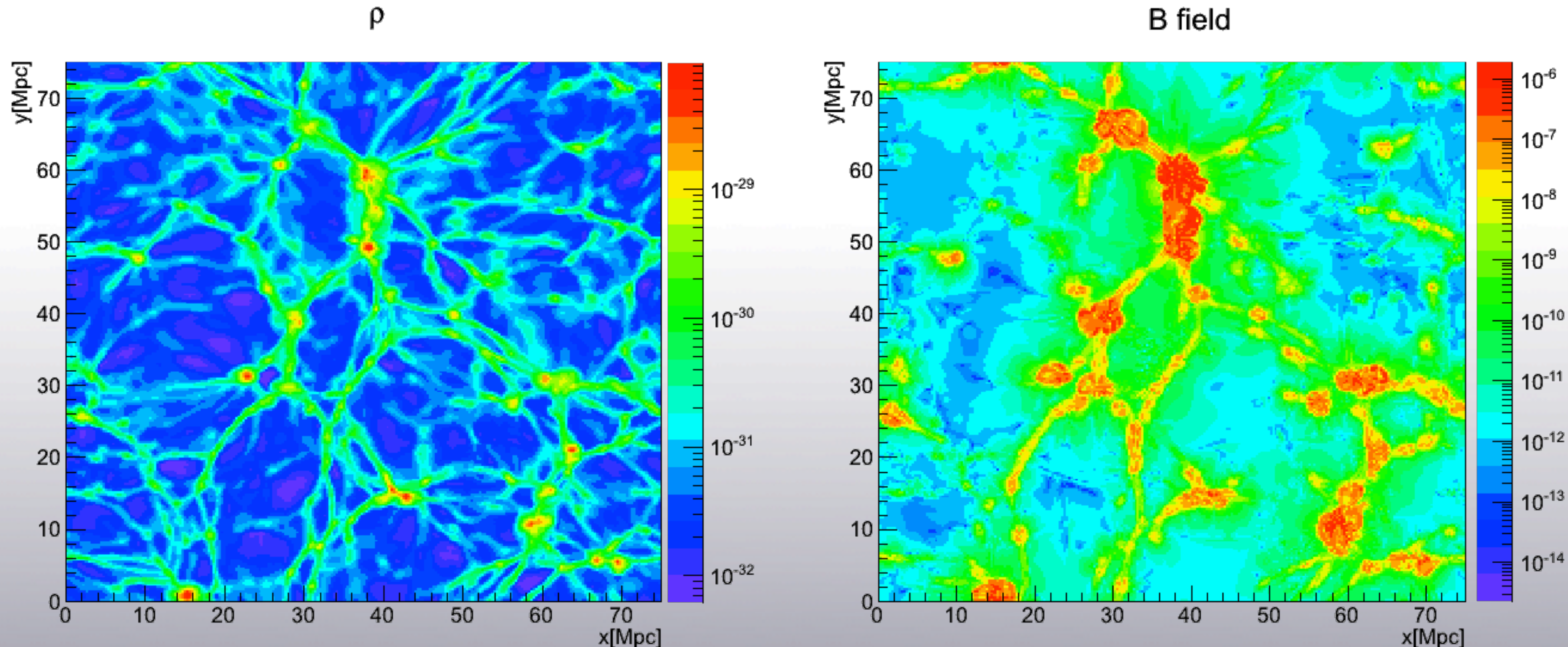

Energy-loss interactions

- Pair production
- Photopion production
- Photodisintegration

} on CMB and EBL

- Nuclear decay
- Redshift losses
- Electromagnetic cascade propagation

R. Alves Batista, D. Boncioli, A. di Matteo, AvV and D. Walz, JCAP 1510 (2015) 10, 063

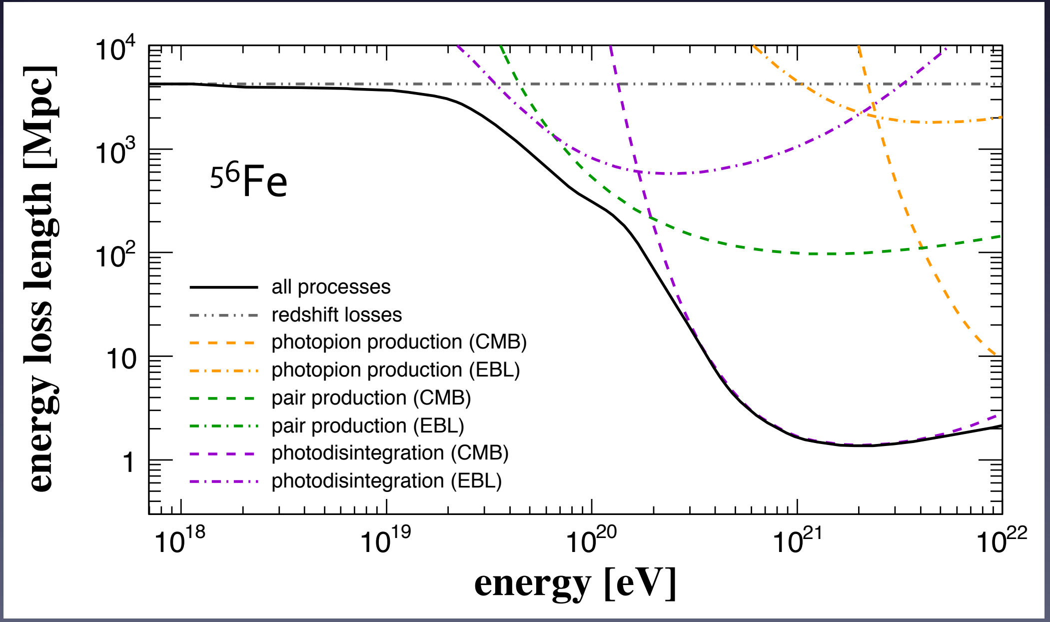

Galactic propagation

- Deflections in the galactic magnetic field
- Example: GMF model by Jansson and Farrar 2012
  - Large-scale regular field
  - Large-scale random (striated) field
  - Small-scale random (turbulent) field

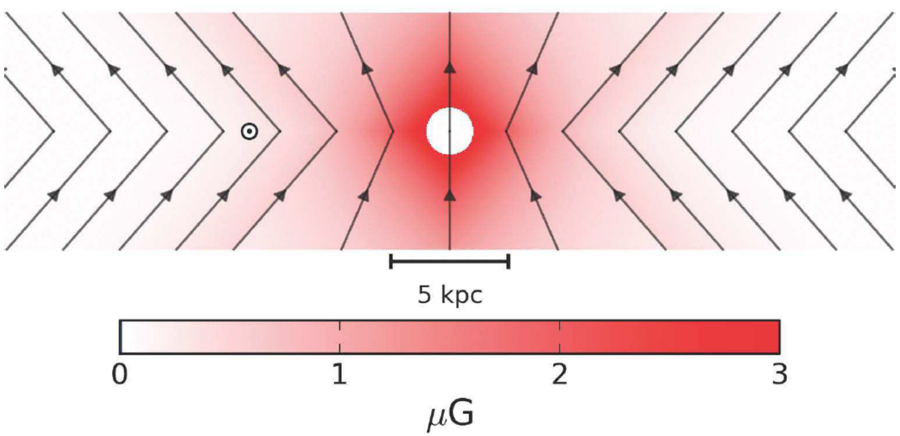

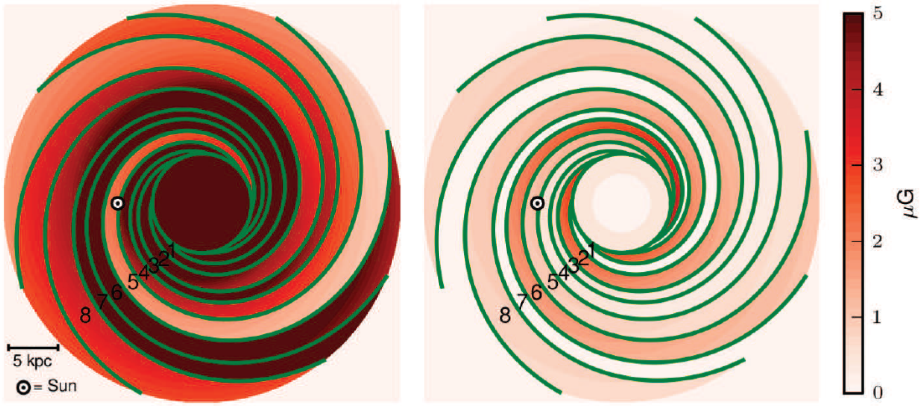

G. Farrar, Comptes Rendus Physique 15 (2014) 339-348

CRPropa 3

R. Alves Batista, A. Dundovic, M. Erdmann, K.-H. Kampert, D. Kümpel, G. Müller, G. Sigl, AvV, D. Walz and T. Winchen, JCAP 1605 (2016) no.05, 038

- A public astrophysical simulation framework for propagating extraterrestrial ultra-high energy particles
- Initial release was on 23/03/2016
- Available from

  crpropa.desy.de
- Online installation on

  VISPA
- Modular redesign of the code structure

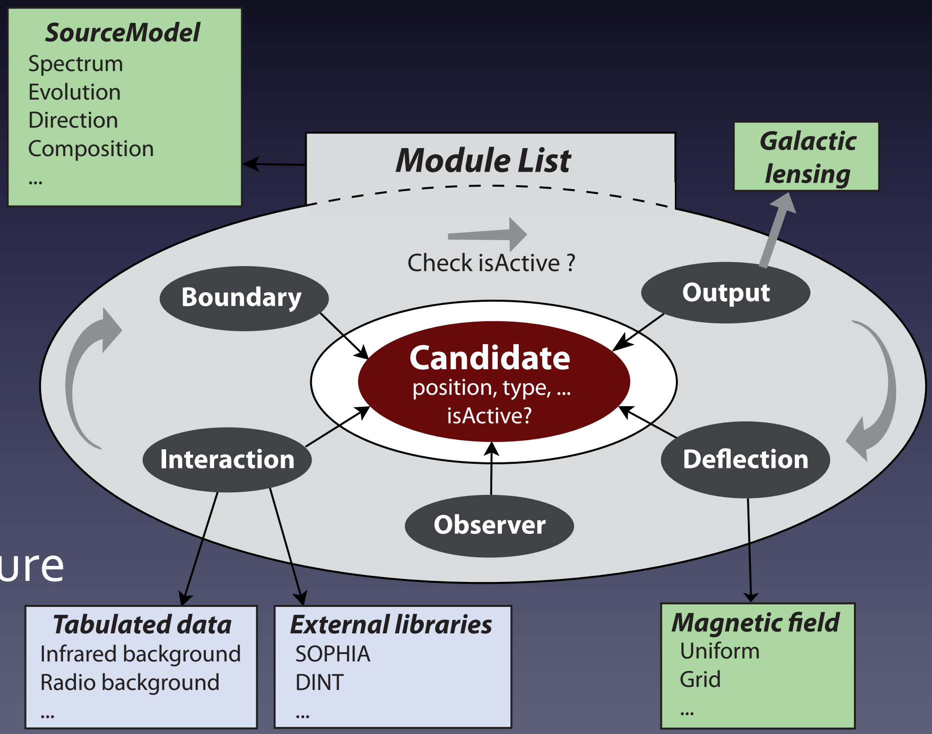

Example simulation

- Source distribution: following LSS from Dolag et al. 2005
- Source density: 10^{-3} Mpc^{-3}
- EGMF structure: Dolag et al. 2005
- EGMF strength: Miniati et al. 2004
- GMF model: Jansson and Farrar 2012
- EBL model: Gilmore et al. 2012
- Injection spectrum: $\frac{\mathrm{d}N}{\mathrm{d}E} \propto \begin{cases} (E/E_0)^{-\alpha}, & E < E_{\mathrm{cut}} \\ (E/E_0)^{-\alpha}\exp(1 - E/E_{\mathrm{cut}}), & E > E_{\mathrm{cut}} \end{cases}$
- Cutoff energy: E_{cut} = 780 EeV
- Injection index: α = 1.5

Arrival directions

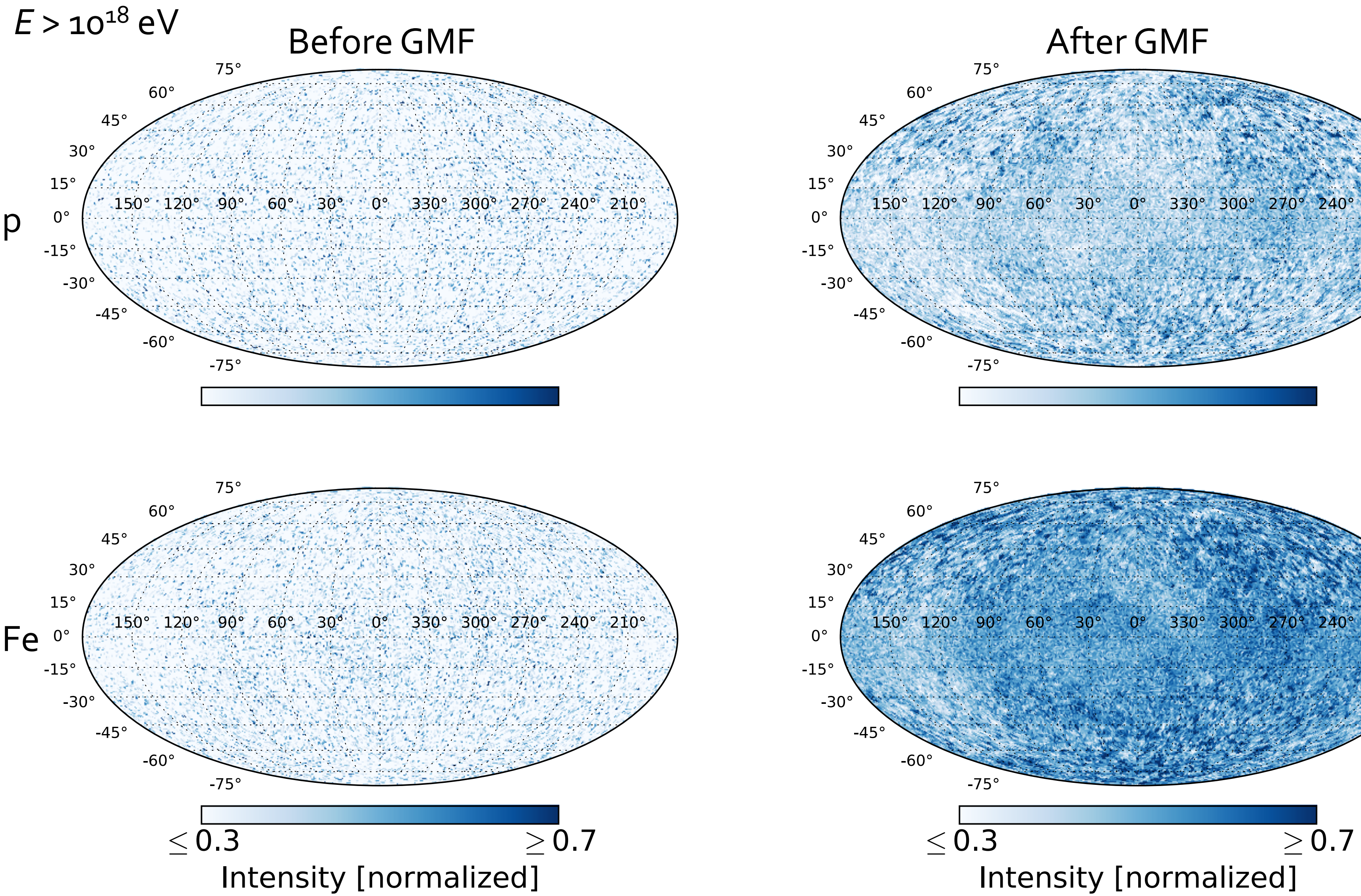

Angular power spectra

- Measure for the anisotropy
- Dipole amplitude: ~0.06
- 99% CL isotropy lines for full sky coverage

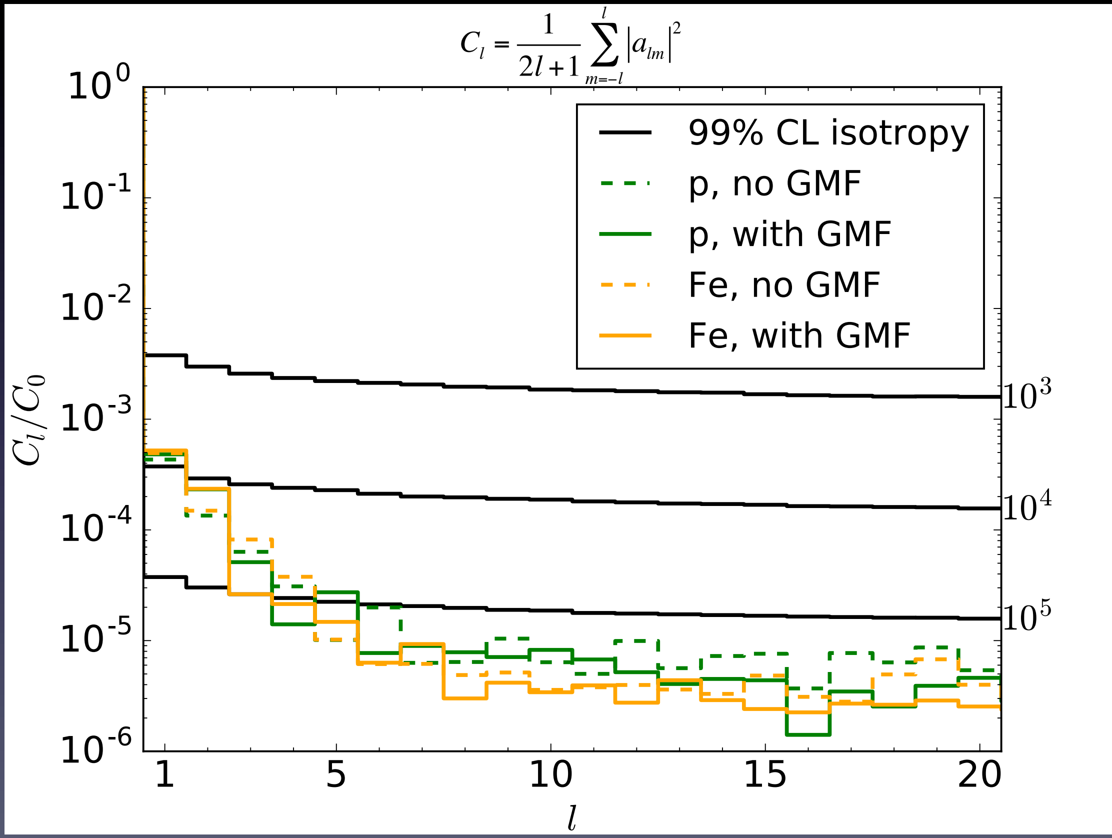

Spectrum and composition

- 4D includes cosmological effects and adiabatic energy losses due to expansion of the universe
- Spectrum: only small differences
- Composition for E<10 EeV:
  - 1D heavier than 4D; increased path length due to EGMF
  - 4D heavier than 3D; adiabatic energy losses

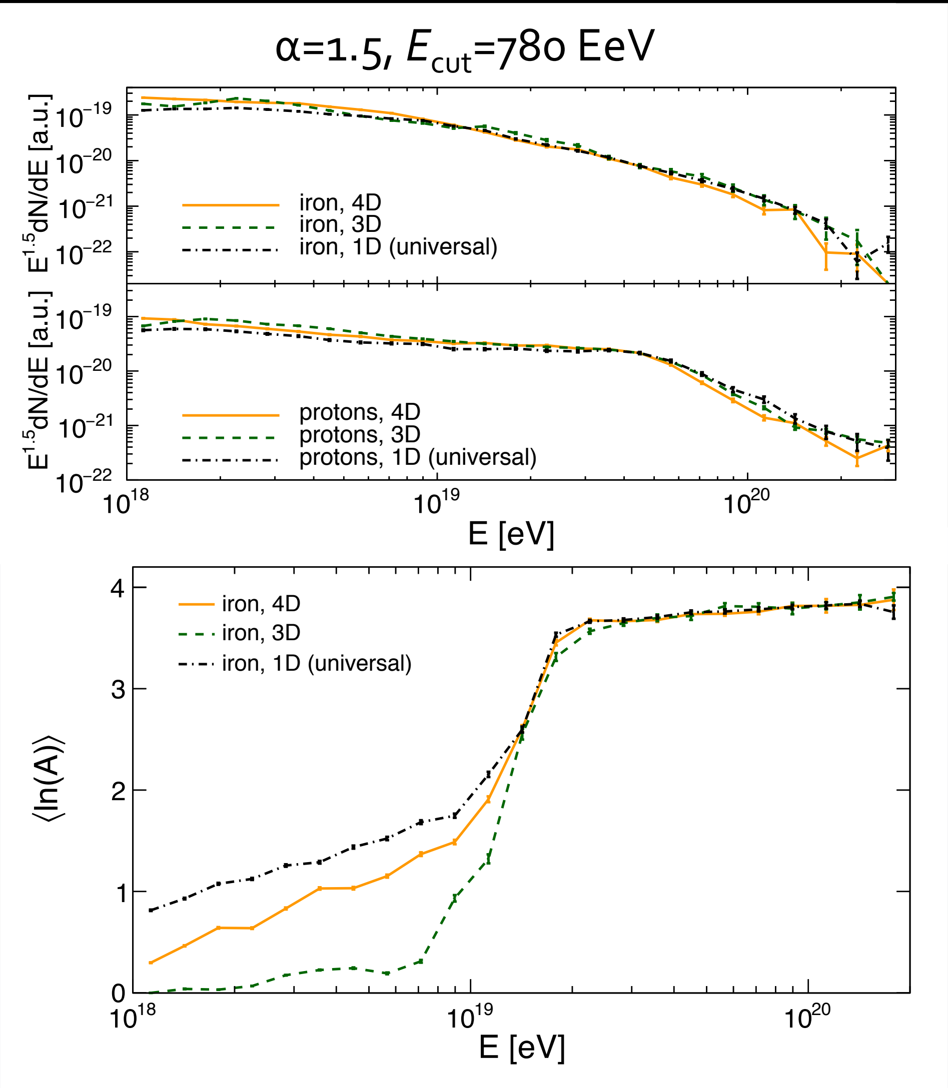

Highly magnetized voids

- MHD simulations of structure formation
- Large differences between EGMF models

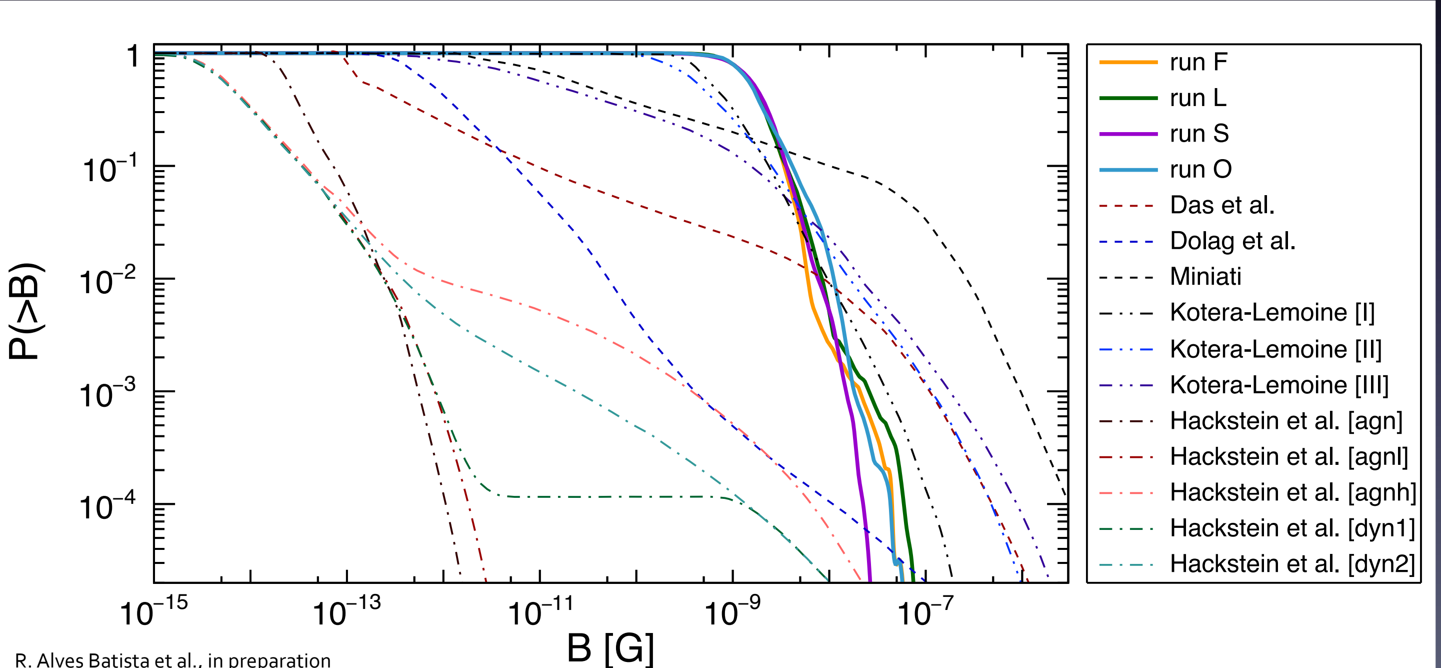

R. Alves Batista et al., in preparation

Average deflections

- Strong magnetic fields in voids
- Deflections of 100 EeV protons closer than ~10 Mpc relatively small (≤ 5°), depending on source distribution and magnetic seed power spectrum
- Deflections of iron nuclei would be very large (≥ 30°) even for nearby sources

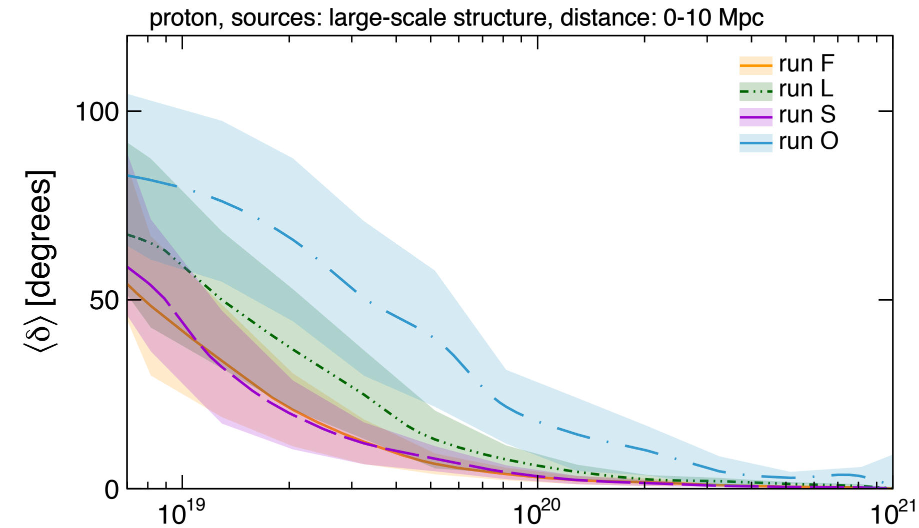

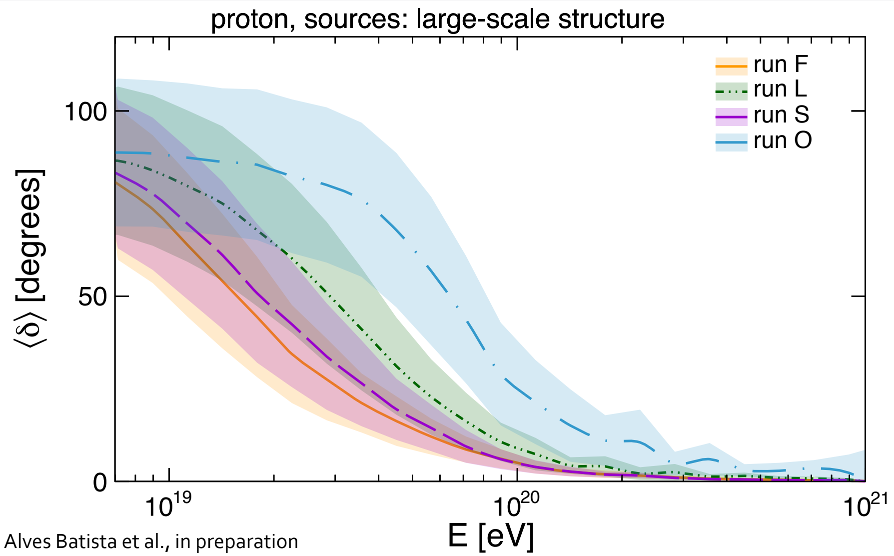

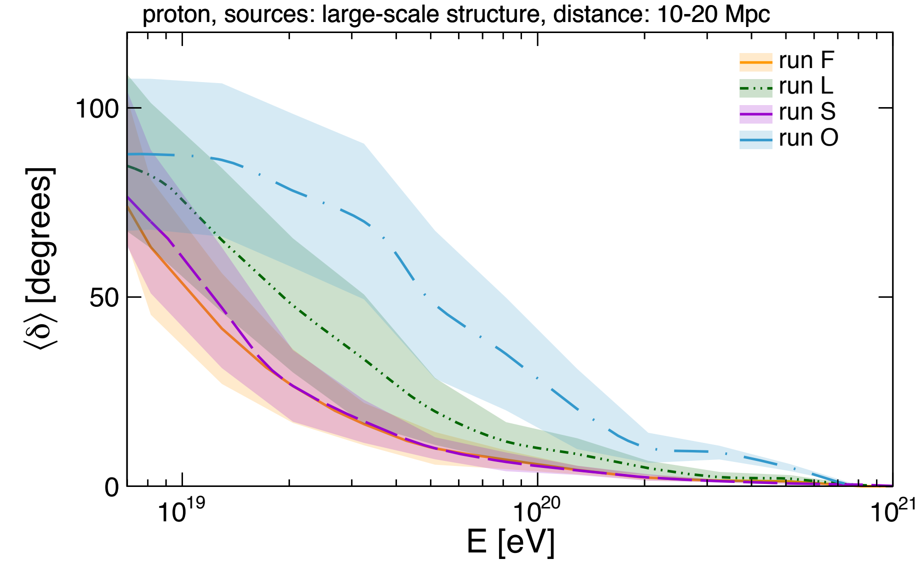

R. Alves Batista et al., in preparation

Full spectrum + composition

- Extragalactic combined fit model + galactic cosmic rays from supernova remnants and Wolf-Rayet star explosions

S. Thoudam, J. P. Rachen, AvV, A. Achterberg, S. Buitink, H. Falcke, J. R. Hörandel, "Cosmic-ray energy spectrum and composition up to the ankle – the case for a second Galactic component", arXiv:1605.03111

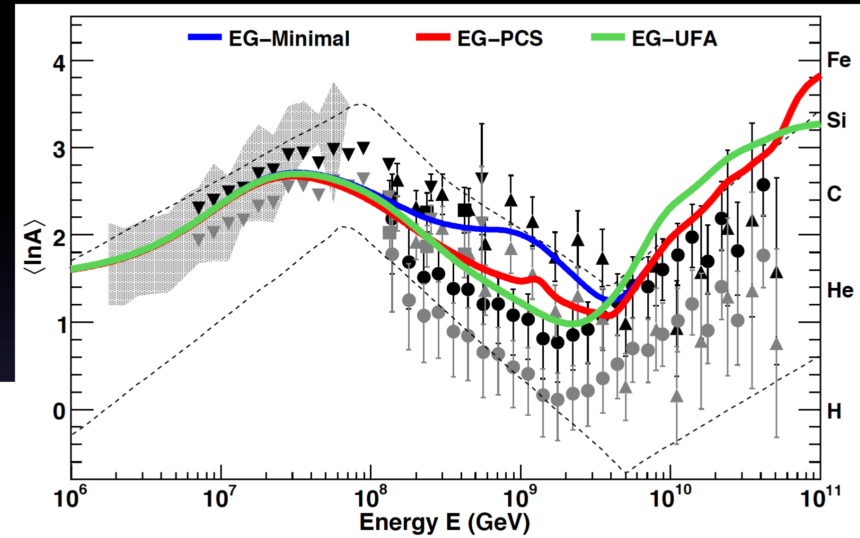

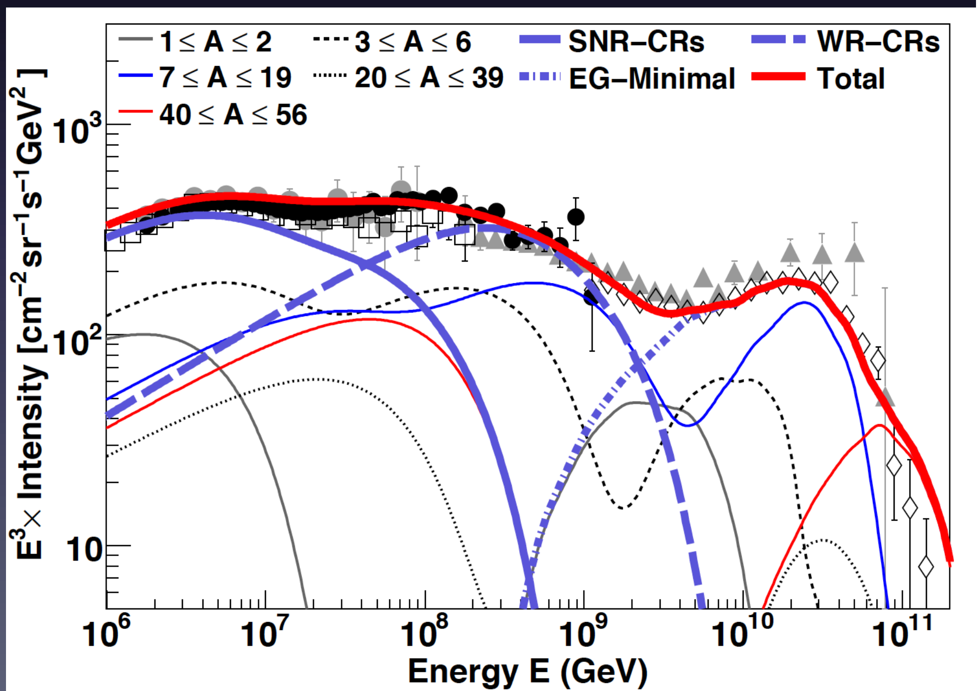

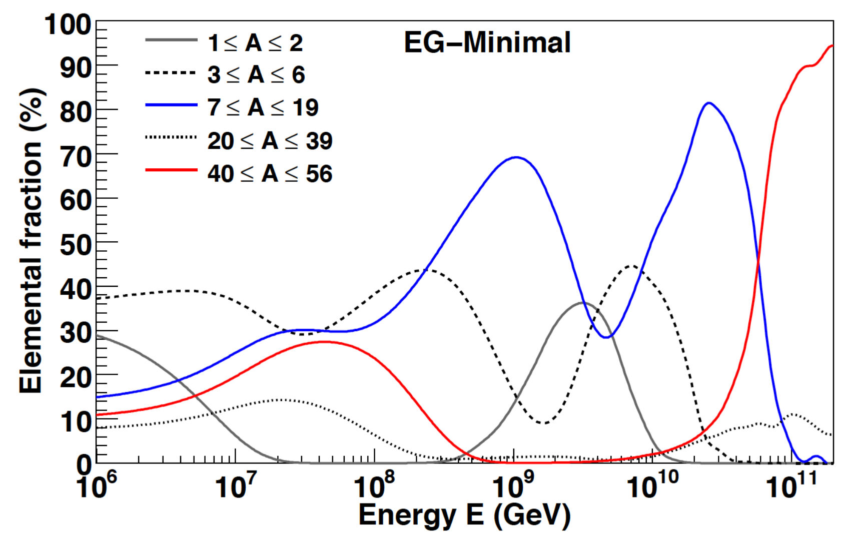

Secondary photons and neutrinos

- Source evolution: GRBs, AGNs, SFR
- ν's and γ's affected strongly
- At tension with Fermi LAT and IceCube results

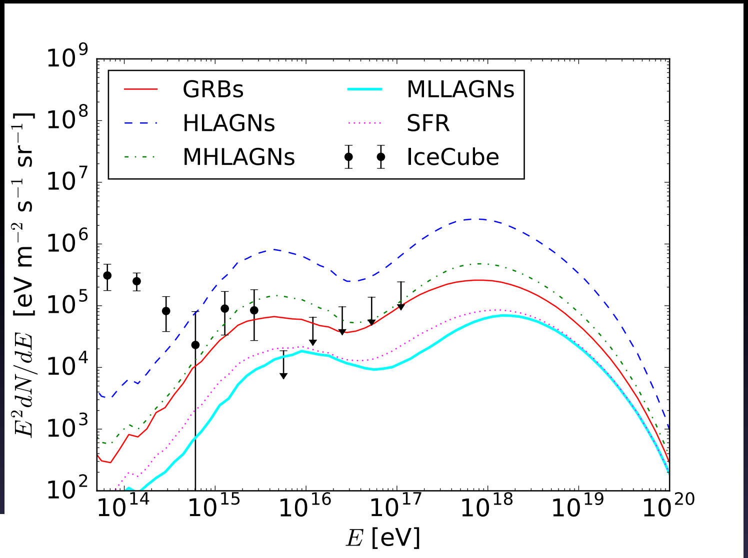

AvV, arXiv:1609.03336

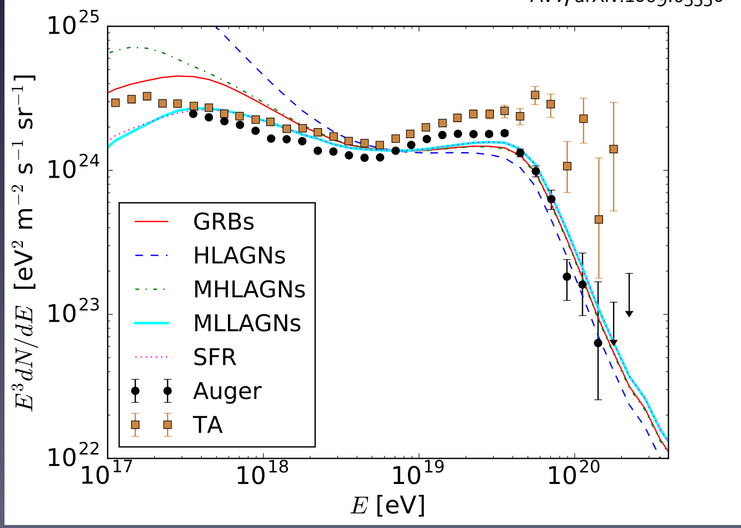

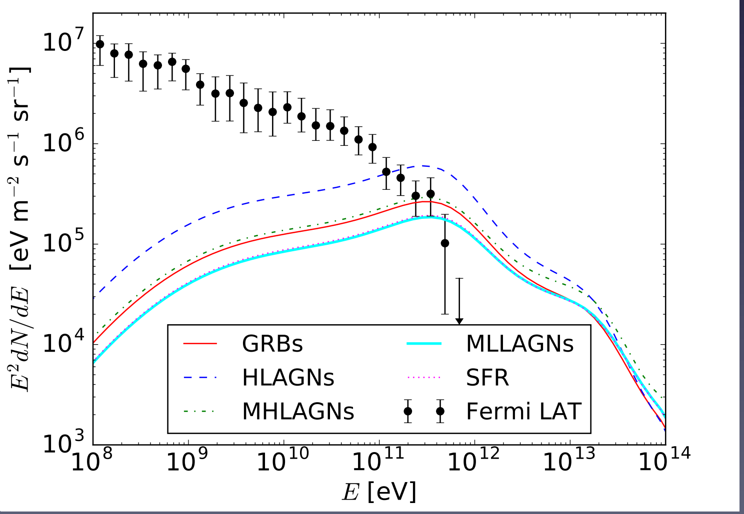

Summary

- CRPropa 3 up and running, available at crpropa.desy.de
- Allows for spectrum, composition and arrival direction predictions for UHECRs as well as for secondary neutrinos and photons
- 3D/4D effects can affect the expected composition
- Expected average deflection at 100 EeV small for protons, but can be large for iron nuclei

Backup slides

1D, 3D and 4D

- 1D:
  - Redshift effects included
  - Magnetic field deflections not included
  - 1D source evolution
  - Particle (almost) always hits observer
- 3D:
  - Redshift effects not included
  - Magnetic field deflections included
  - 3D source distribution
  - Particle can miss observer in space
- 4D:
  - Redshift effects included
  - Magnetic field deflections included
  - 3D source distribution + evolution
  - Particle can miss observer in space and time

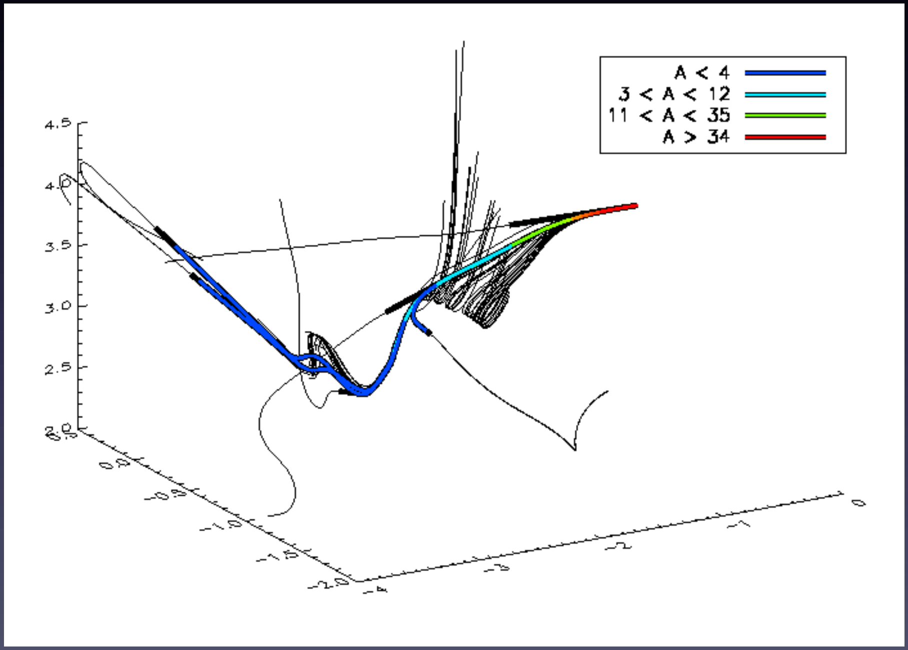

Reference scenario

- Homogeneous distribution of identical sources
- Injection spectrum: $\frac{\mathrm{d}N}{\mathrm{d}E} \propto E^{-\alpha} \exp(-E / ZR_{\mathrm{cut}})$
- Maximum energy: R_{cut} = Z*200 EV
- Injection index: $\alpha = 2.5$
- Source evolution: comoving
- Initial CR type: protons

Reference scenario

- Already some tension with Fermi LAT isotropic diffuse γ-ray background

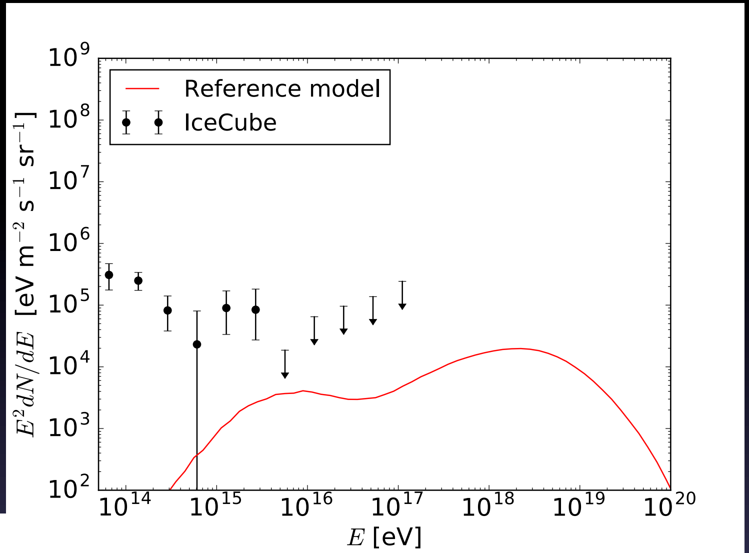

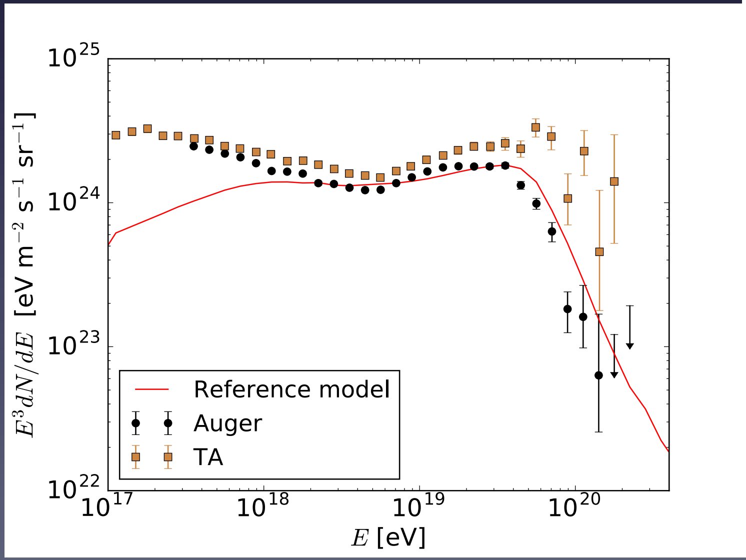

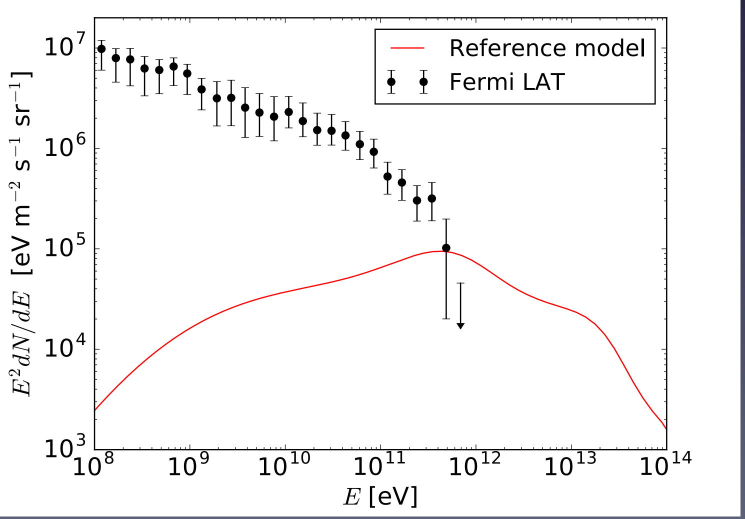

Maximum energy dependence

- 50 ≤ R_{cut} ≤ 800 EV
- ν's only affected for E>10 EeV
- γ's only slightly affected

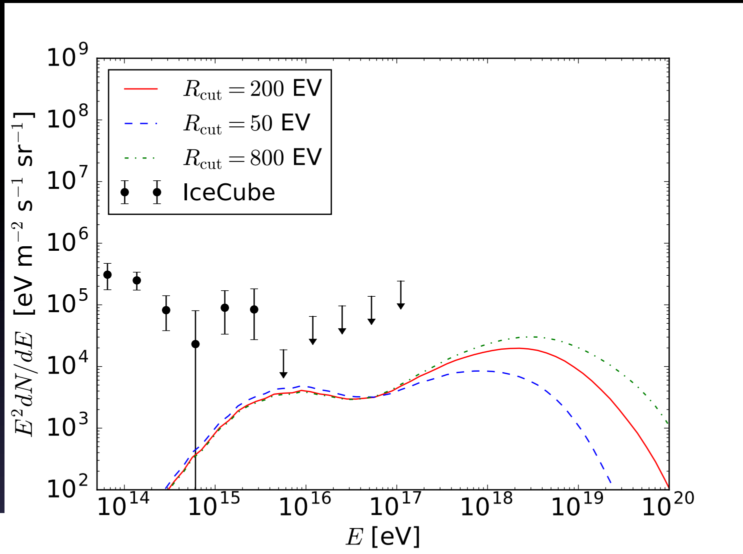

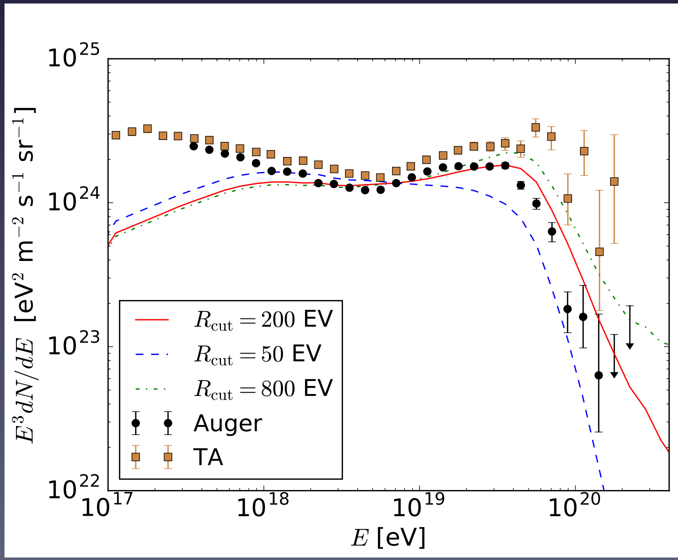

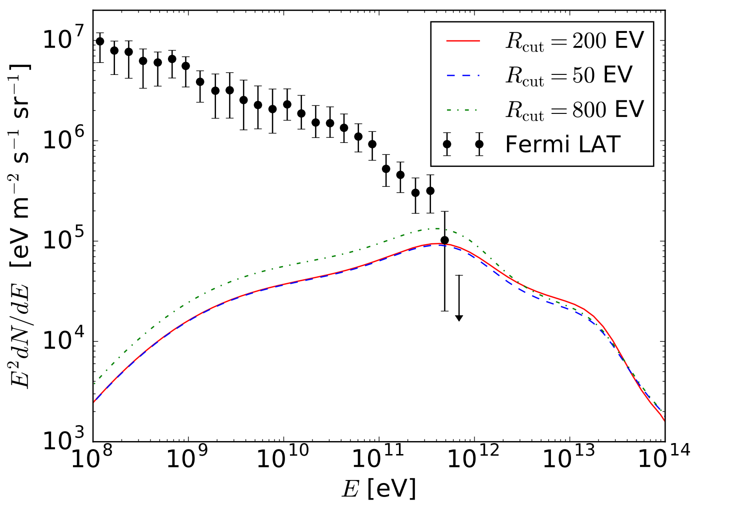

Spectral index dependence

- $2.0 \leq \alpha \leq 2.9$
- ν's affected similarly as CRs
- γ's only slightly affected

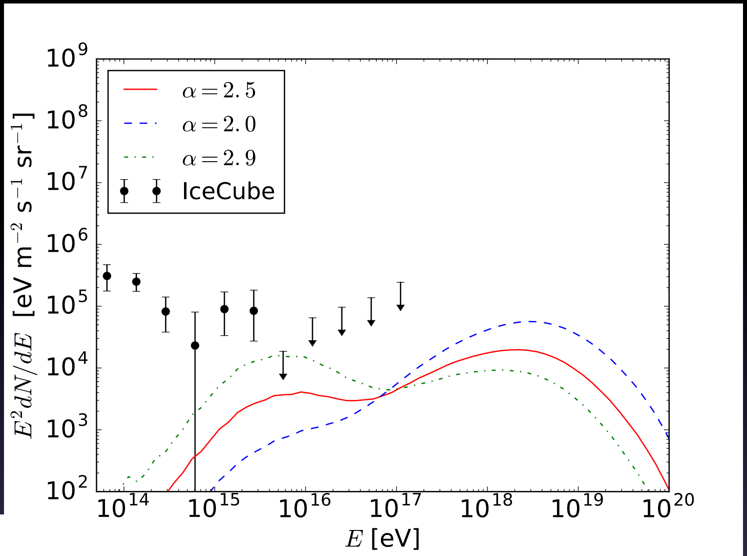

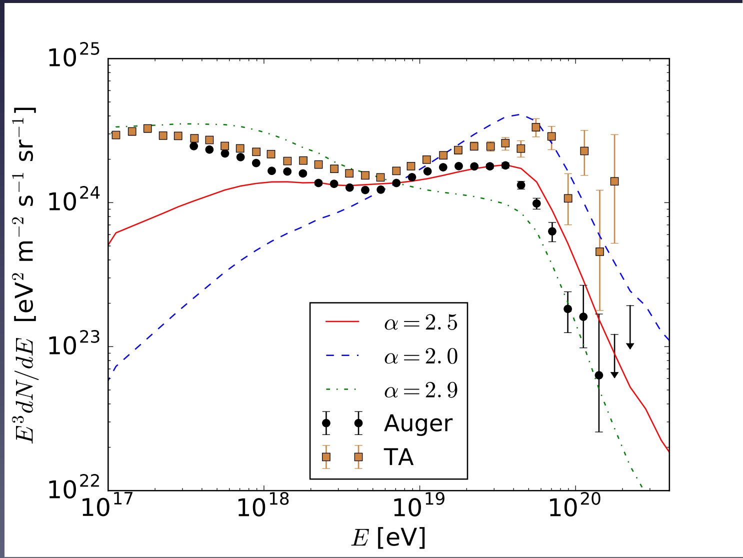

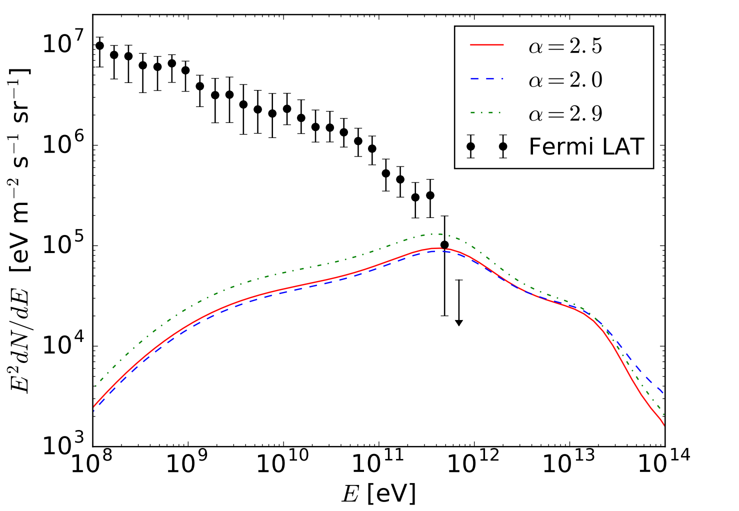

Source evolution dependence

- Multiplied by $(1+z)^m$, for $-6 \leq m \leq 6$
- m = 0: BL Lacs
- m = -6: HSP BL Lacs
- ν's and γ's affected strongly
- Only $m \approx -6$ allowed by Fermi LAT

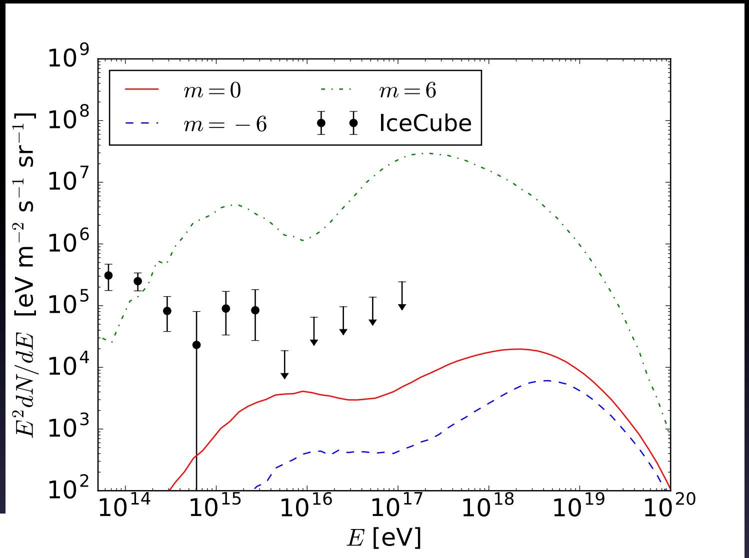

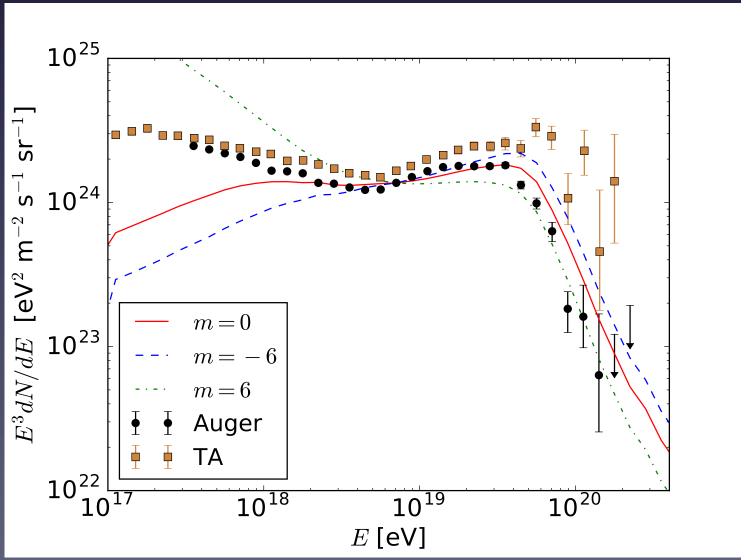

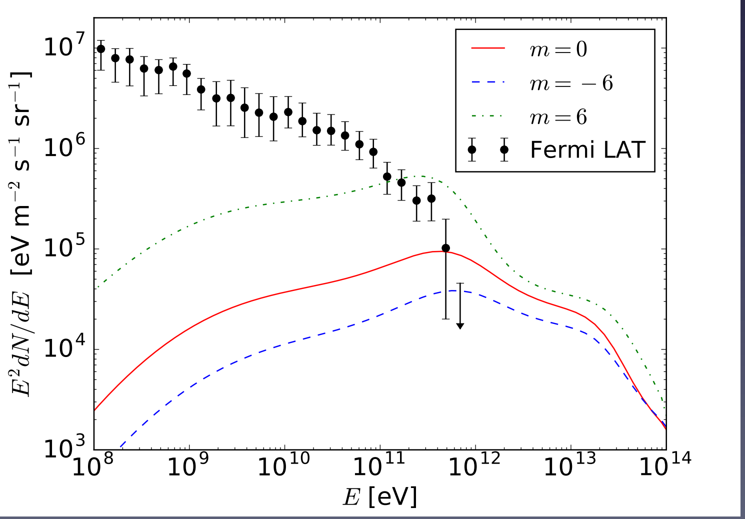

Source evolution models

- GRBs, AGNs, SFR
- ν's and γ's affected strongly
- None allowed by Fermi LAT

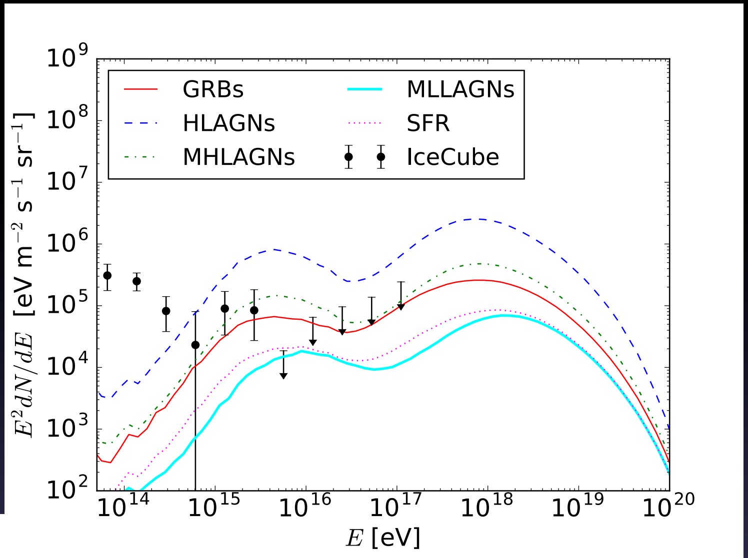

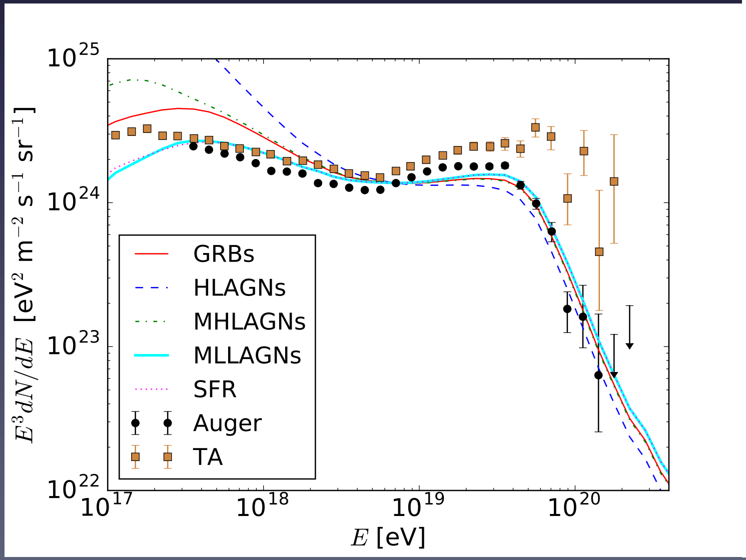

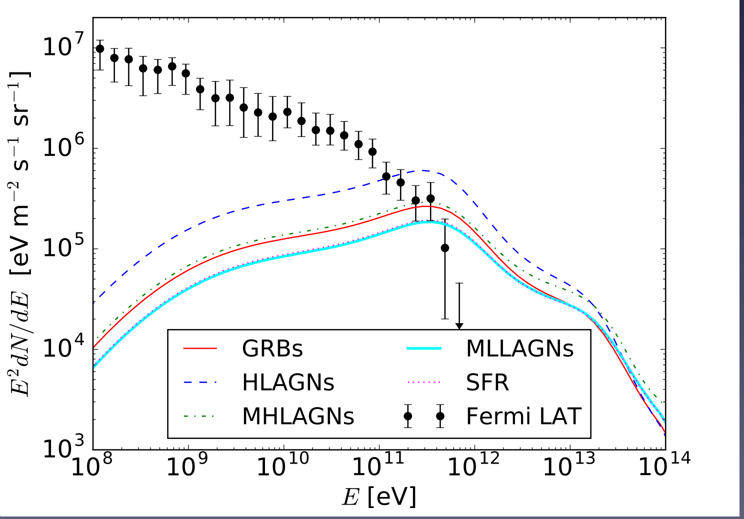

CR mass dependence

- Initial CR: protons vs iron
- Heavier primaries reduces neutrino and photon flux

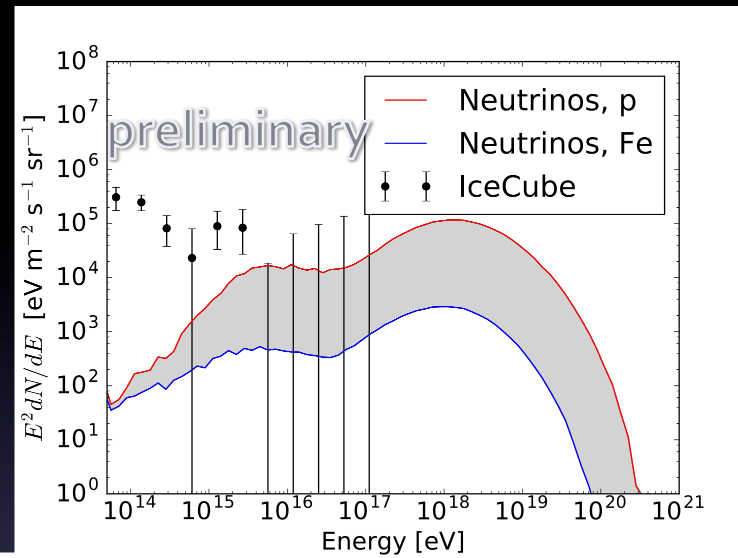

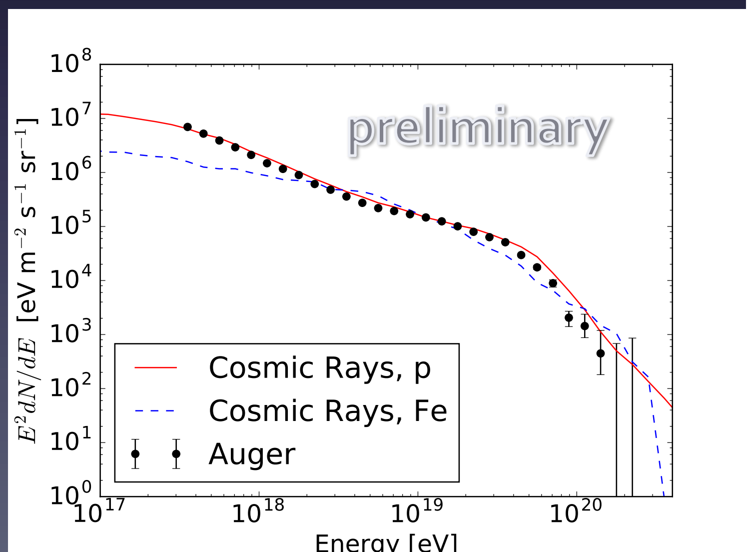

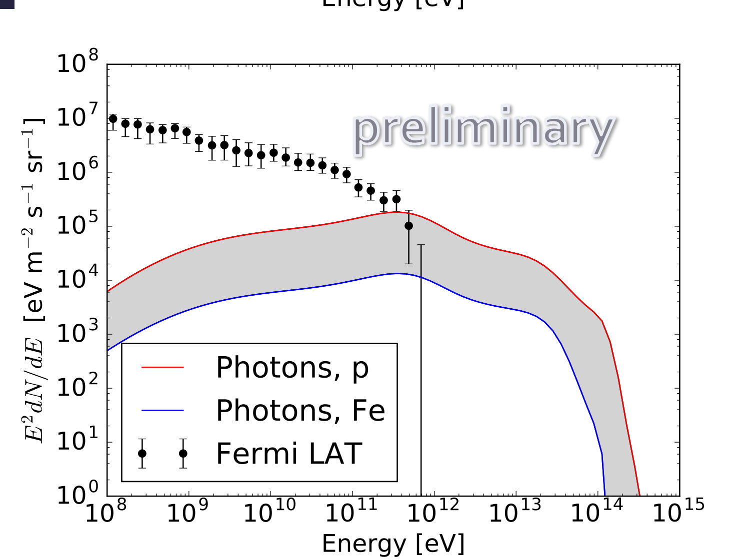

1D: Combined fit

$$\frac{dN}{dE} \propto \begin{cases} p_i E^{-\gamma}, & E/Z_i < R_{cut} \\ p_i E^{-\gamma}\exp(1 - E/Z_i R_{cut}), & E/Z_i > R_{cut} \end{cases}$$

$$\gamma = 0.94^{+0.09}_{-0.10}$$

$$\log_{10}(R_{cut}/V) = 18.67 \pm 0.03$$

$$p_H = 0.0^{+29.9}\%$$

$$p_{He} = 62.0^{+3.5}_{-22.2}\%$$

$$p_N = 37.2^{+4.2}_{-12.6}\%$$

$$p_{Fe} = 0.8^{+0.2}_{-0.3}\%$$

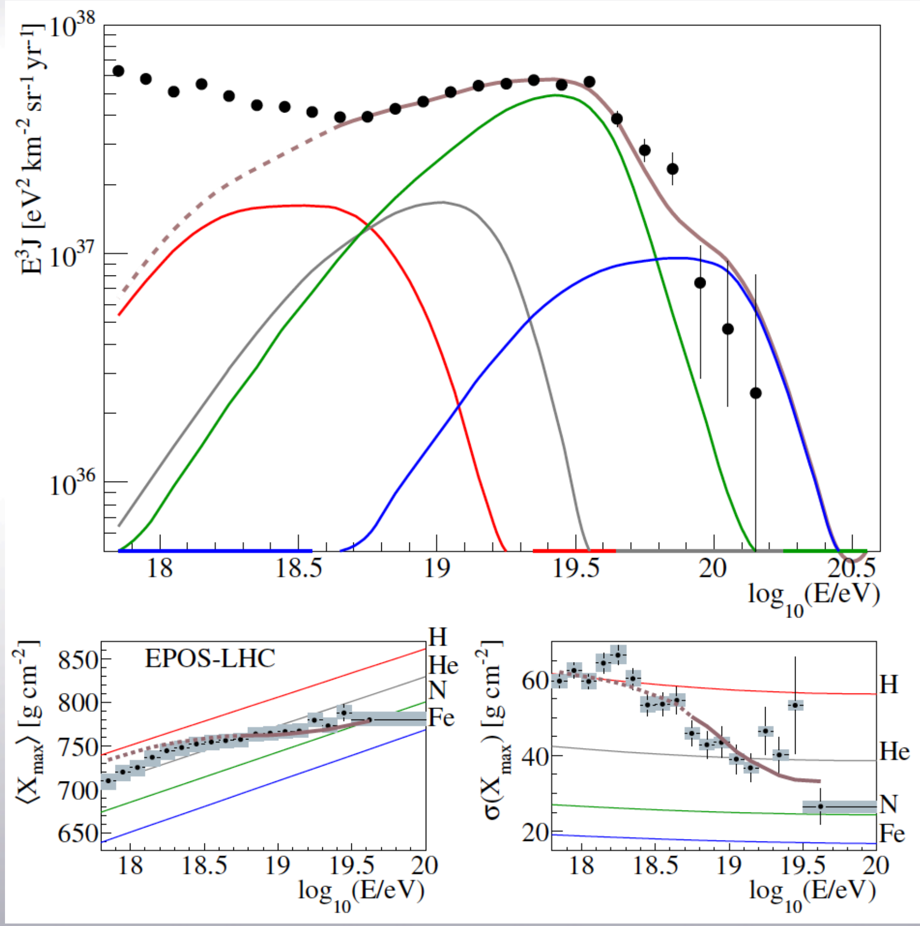

Auger, arXiv:1509.03732

Mixed composition combined fit

- By di Matteo et al. for the Pierre Auger Collaboration, arXiv:1509.03732
- Comoving source evolution
- $\gamma = 0.73$
- $R_{max} = 3.8$ EV
- 98.69% Nitrogen, 1.31% Iron

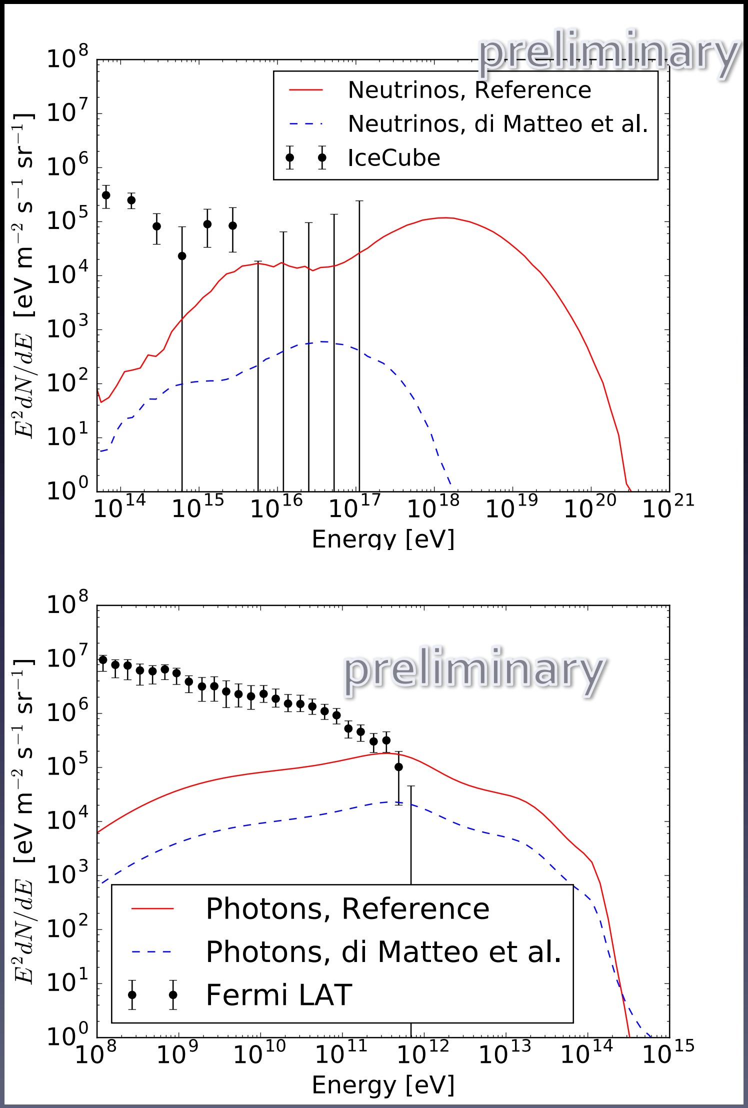

Pair production

$$^{A}\mathrm{N} + \gamma \rightarrow {}^{A}\mathrm{N} + e^{+} + e^{-}$$

- Energy loss per interaction ~$2m_e/m_p \approx 0.1\%$

  $\rightarrow$ continuous energy loss

- Most important reaction for creation of secondary photons in the TeV range

Photopion production

$$^{\mathrm{A}}\mathrm{N} + \gamma \rightarrow {}^{\mathrm{A\text{-}1}}\mathrm{N}' + p + \pi^0 \rightarrow {}^{\mathrm{A\text{-}1}}\mathrm{N}' + p + \gamma\gamma$$
$$\rightarrow {}^{\mathrm{A}-1}\mathrm{N}' + n + \pi^+$$

- Event generation, mean free path and energy loss from SOPHIA
- “Simulates the interactions of nucleons with photons over a wide range in energy”
- “The simulation of the final state includes all interaction processes which are relevant to astrophysical applications”
- “Includes resonance excitation and decay, direct single pion production and diffractive and non–diffractive multiparticle production”

Photodisintegration and decay

$$ {}^{A}\mathrm{N} + \gamma \rightarrow {}^{A'}\mathrm{N'} + X(n, p, \ldots) $$

- PD cross sections for 183 isotopes from TALYS + extensions for A<12, 2200 excl. channels
- All isotopes with lifetime >2s, A≤56 and Z≤26
- Nuclear decay for 434 isotopes from NuDat2 + alterations to correctly account for electron capture

Photon backgrounds

- CMB
- EBL, 6 different models

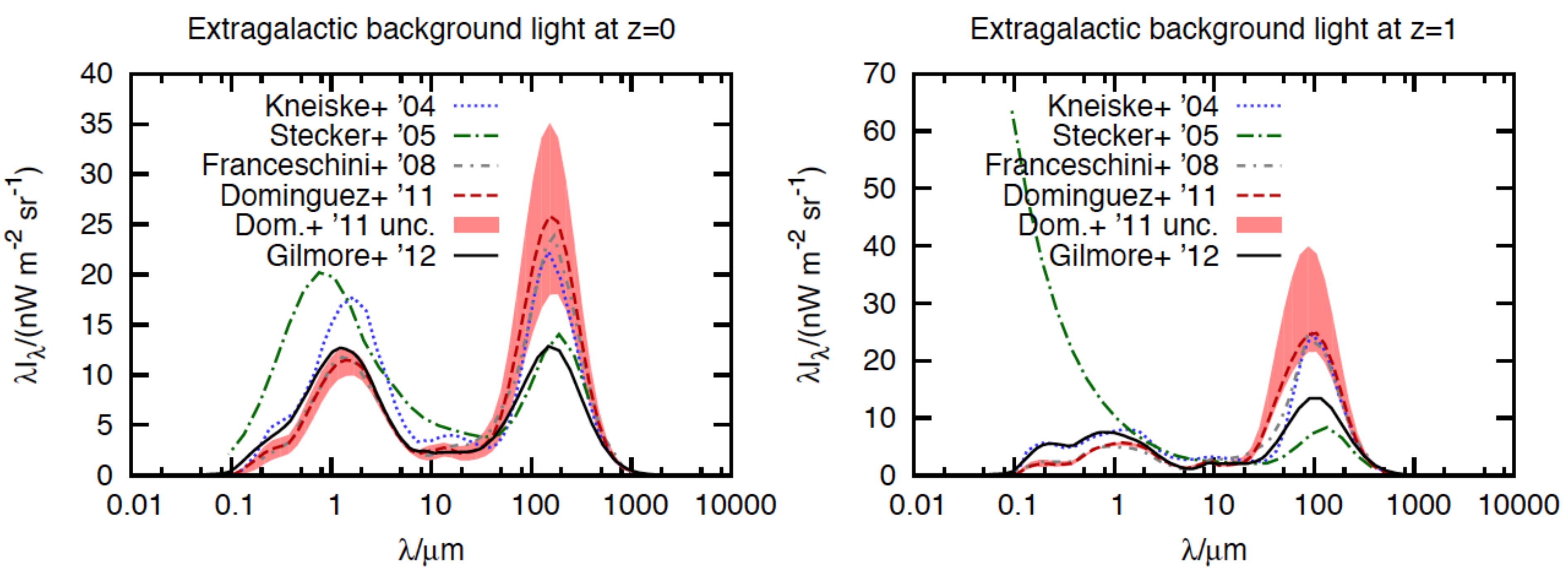

Galactic propagation

- Cosmic ray propagation through magnetic fields can be modelled on any scale
- From the CRPropa 3 paper:

General magnetic fields	
Uniform	Magnetic field is a position independent single vector magnetic field.
Grid	Provides a periodic magnetic field grid with trilinear interpolation, equal spacing, and different sizes along each axis.
Modulated Grid	Modulates a large scale vector field by a periodic small scale scalar field.
Turbulent	A random magnetic field with a turbulent spectrum [23].

Galactic magnetic fields	
Toroidal Halo	Toroidal halo field model adopted from [24, 25].
Logarithmic Spiral	Magnetic field model of axisymmetric (ASS) or bisymmetric (BSS) logarithmic spiral shape.
Pshirkov 2011	Pshirkov et al. magnetic field model, consisting of a large-scale regular (disk and halo) field [16]. The axisymmetric (ASS) and the bisymmetric (BSS) disk model can be chosen.
JF 2012	Implementation of the Jansson & Farrar magnetic field model, consisting of a large-scale regular and random (striated) field and a small-scale random (turbulent) field [10, 15].

3D: Lensing method

- Lenses obtained through backtracking
- Stored in matrices dependent on rigidity *E/Z*
- Map discrete directions outside the galaxy to discrete observed directions on Earth

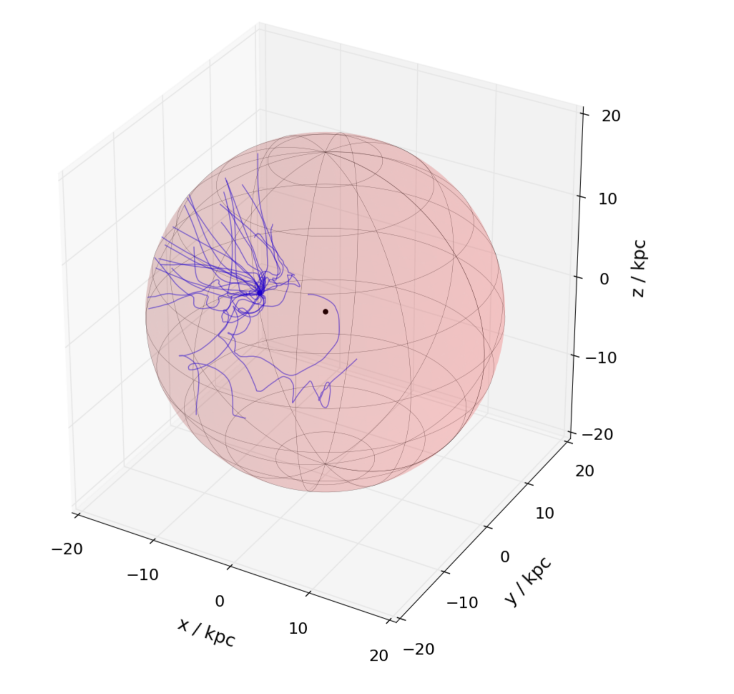

Galactic lensing method

- Map discrete directions outside the galaxy to discrete observed directions on Earth

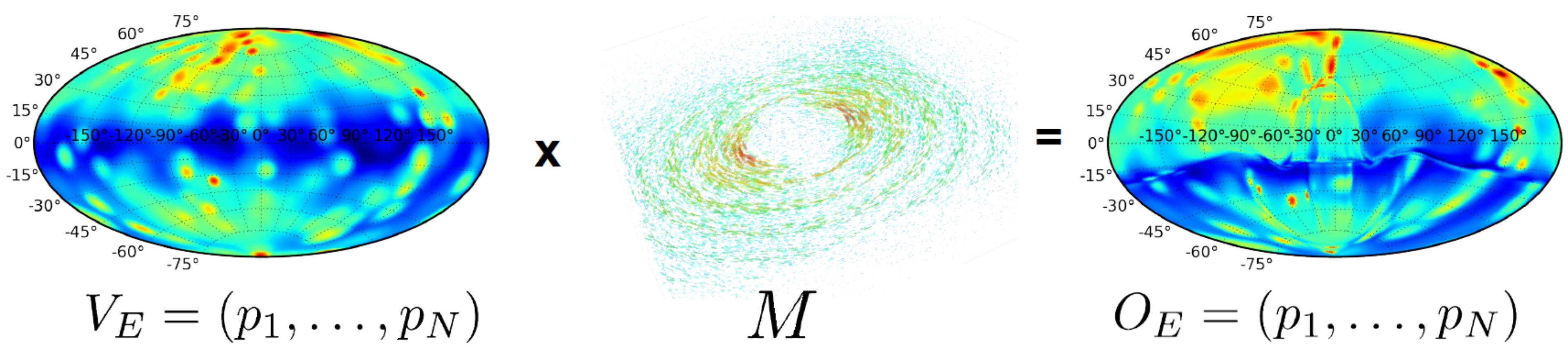

Galactic deflection matrix

- Backtrack ~10^6 UHECRs per rigidity, 100 rigidity bins

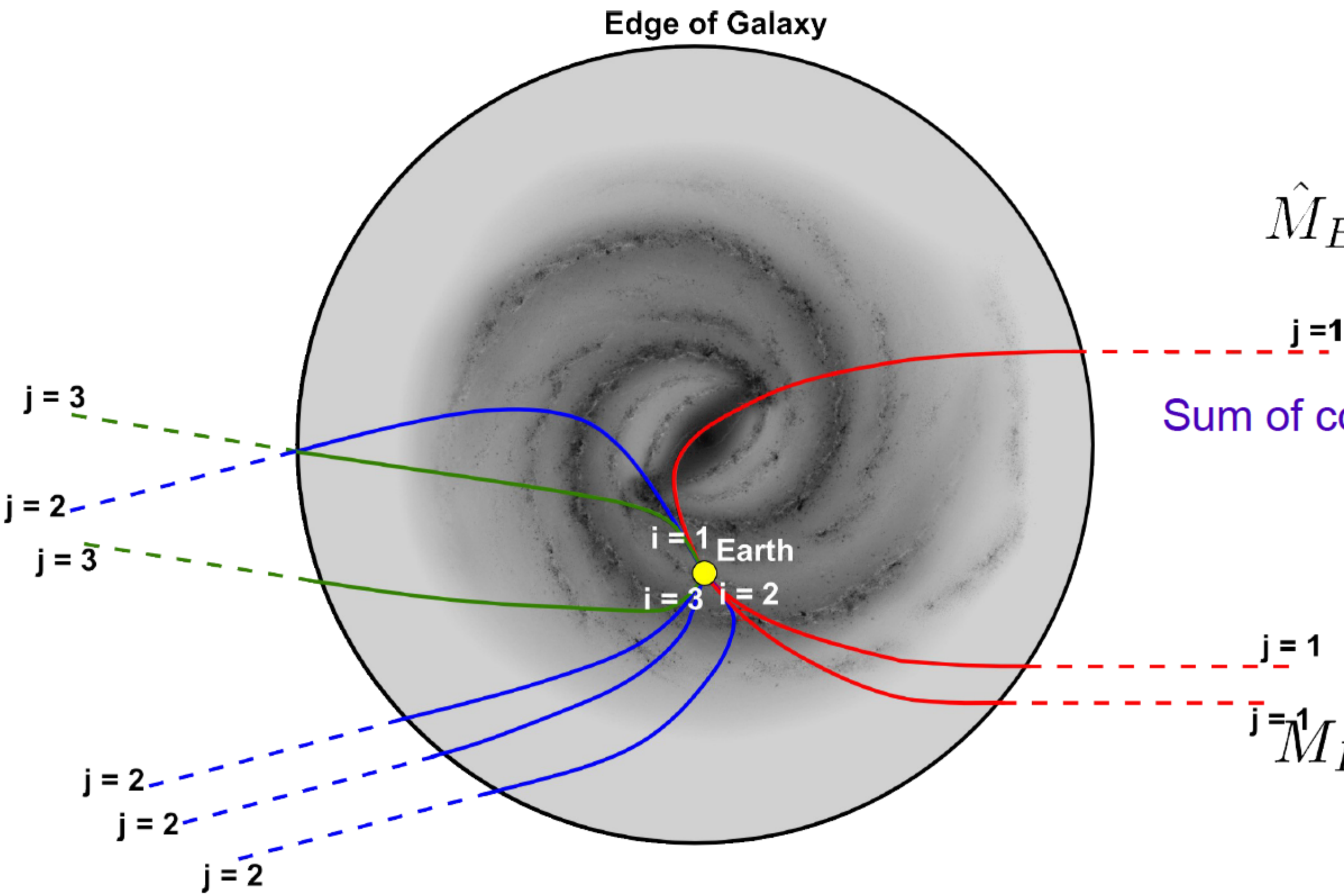

$$\hat{M}_E = \begin{pmatrix} 1 & 1 & 1 \\ 2 & 1 & 0 \\ 0 & 2 & 1 \end{pmatrix}$$

(j →, i ↓)

Sum of columns 3 4 2

$$M_E = \begin{pmatrix} \frac{1}{4} & \frac{1}{4} & \frac{1}{4} \\ \frac{2}{4} & \frac{1}{4} & 0 \\ 0 & \frac{2}{4} & \frac{1}{4} \end{pmatrix}$$

Galactic deflection matrix

2/3 of flux eneter galaxy in pixel 1
1/3 of flux enter galaxy in pixel 2

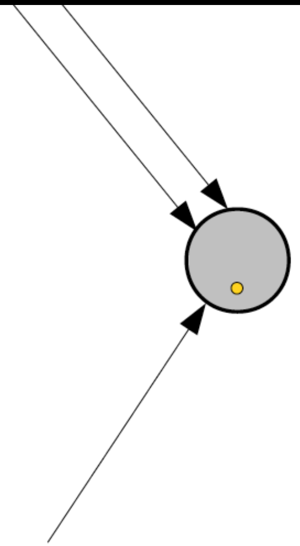

$$\vec{v} = \begin{pmatrix} \frac{2}{3} \\ \frac{1}{3} \\ 0 \end{pmatrix}$$

j →, i ↓

$$M_E = \begin{pmatrix} \frac{1}{4} & \frac{1}{4} & \frac{1}{4} \\ \frac{2}{4} & \frac{1}{4} & 0 \\ 0 & \frac{2}{4} & \frac{1}{4} \end{pmatrix}$$

$m_{i,j}$ is probability that particle which enters galaxy in pixel *j* is observed on earth in pixel *i*

Get observed distribution by matrix multiplication

$$M_E \cdot \vec{v} = \vec{o}$$

$$\begin{pmatrix} \frac{1}{4} & \frac{1}{4} & \frac{1}{4} \\ \frac{2}{4} & \frac{1}{4} & 0 \\ 0 & \frac{2}{4} & \frac{1}{4} \end{pmatrix} \cdot \begin{pmatrix} \frac{2}{3} \\ \frac{1}{3} \\ 0 \end{pmatrix} = \begin{pmatrix} \frac{3}{12} \\ \frac{5}{12} \\ \frac{2}{12} \end{pmatrix}$$

Uncertainties

R. Alves Batista, D. Boncioli, A. di Matteo, AvV and D. Walz, "Effects of uncertainties in simulations of extragalactic UHECR propagation, using CRPropa and SimProp", JCAP 1510 (2015) no.10, 063, arXiv:1508.01824

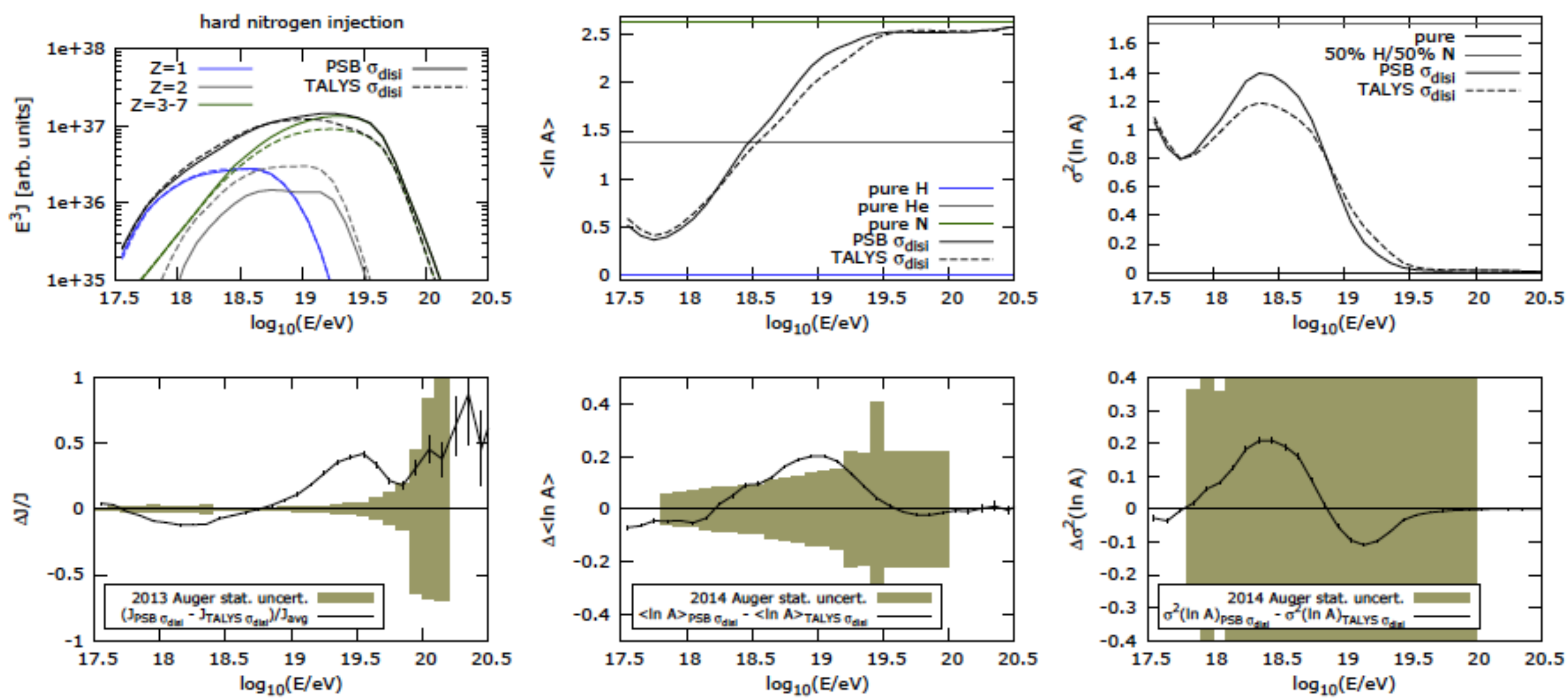

Figure 8. Comparison of PSB and TALYS photodisintegration models for hard nitrogen injection.

EGMF constrains

G. Sigl, *"Astroparticle Physics: Theory and Phenomenology"*

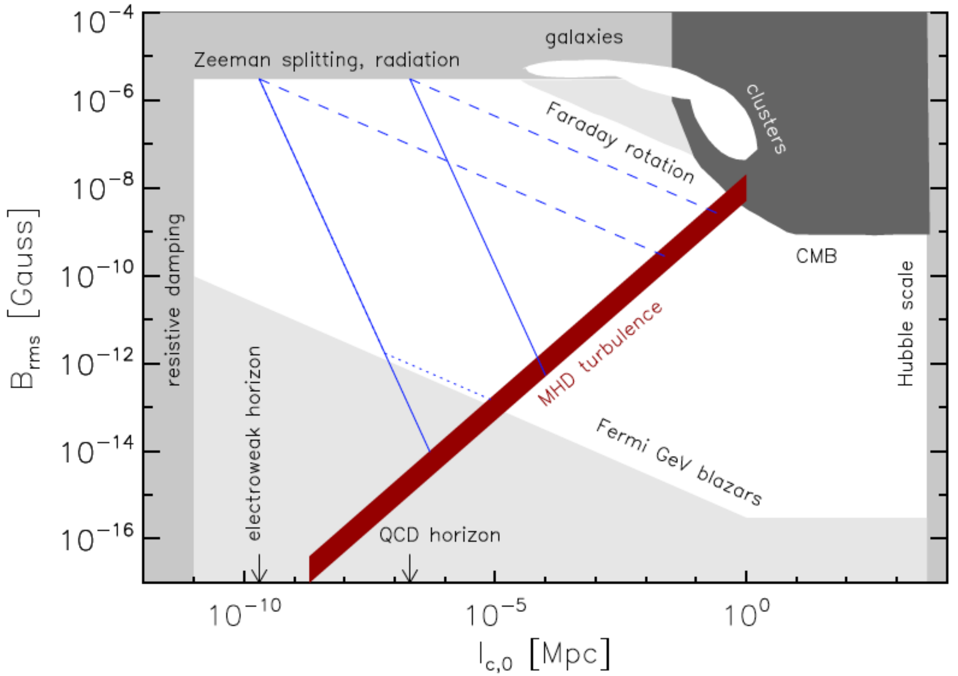

Fig. 4.8 Summary of observational constraints on cosmological fields in the plane of comoving coherence length and r.m.s. field strength are presented as shaded areas. At lengths below the resisitive length scale given by Eq. (4.130) magnetic fields would be damped within a Hubble time, the CMB constraint is from Ref. [181], the Faraday rotation limits are from Ref. [178, 179], the horizontal upper limit is from the contribution to radiation, see Eq. (4.194), and the Zeeman effect on spectral lines, and the coherence length can not be larger than today's Hubble scale. A possible lower limit of the form of Eq. (8.79) [182] (Fermi GeV blazars) will be discussed in Sect. 8.1.8, but is not generally agreed upon. Magnetic fields in galaxies and galaxy clusters are shown as white shades. The relation Eq. (4.141) for MHD turbulence is shown as red band. Dashed and solid blue lines show the evolution of maximally helical and non-helical fields following Eq. (4.146) and (4.148), respectively, with initial comoving strength 3×10^{-6} G and coherence length given by the comoving Hubble scale at the electroweak and QCD phase transition, see Eq. (4.121), shown as arrows. The dotted blue line is for initial magnetic helicity $H_i = 10^{-10} H_{\max}$ starting at the electroweak scale, motivated by certain baryogenesis scenarios discussed in Sect. 4.7 below. Since helicity is conserved, see Eq. (3.272), it follows the non-helical scaling until $B_0^2 l_{c,0}$ has decreased by a factor $H_i/H_{\max}$ after which the field is maximally helical and follows the scaling Eq. (4.146). Parts of figure based on Ref. [182].

Initial magnetic field

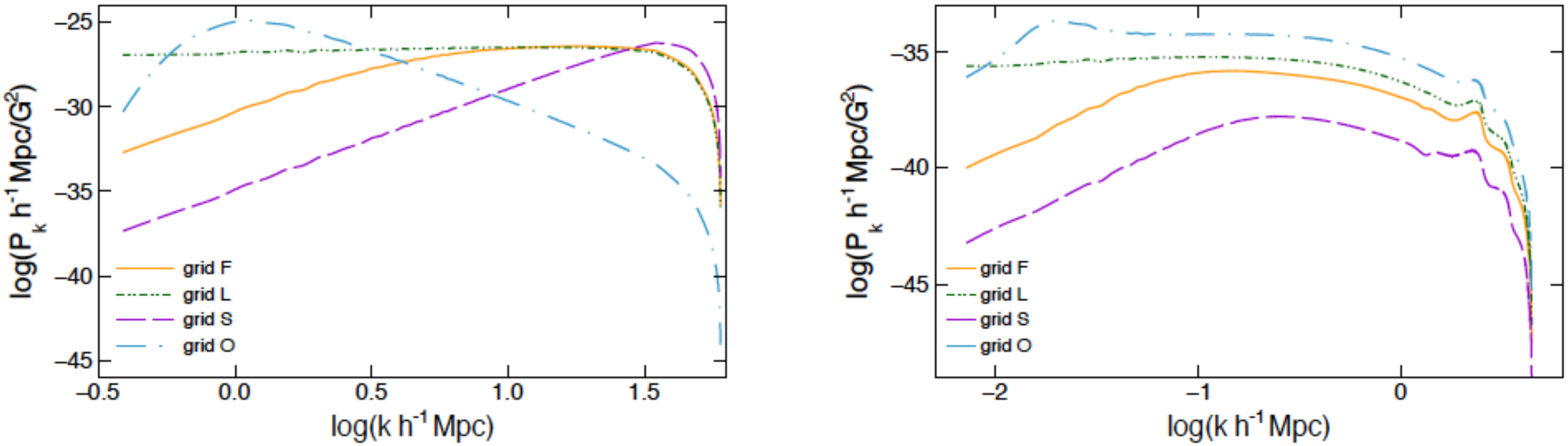

FIG. 1. Power spectrum of the initial magnetic field at $z \simeq 53$ (left) and $z \approx 0$ (right panel), in comoving units, as a function of the comoving wave number $h^{-1}k$.

Alves Batista et al., in preparation

Spectra of EGMF paper

The propagation was done using the CRPropa 3 code [51]. Particles are injected by sources with energies between 1 EeV and 1000 EeV, with the following spectrum

$$\frac{dN}{dE} \propto \begin{cases} E^{-\alpha} & \text{if } E_{max} > E \\ E^{-\alpha} \exp\left(1 - \frac{E}{E_{max}}\right) & \text{if } E_{max} \leq E \end{cases}, \quad (1)$$

where $\alpha_{\rm Fe} = 1$ and $\alpha_{\rm p} = 2$ are the spectral indices for the injected iron and proton scenarios, respetively. Here E_{max} is the maximal energy. In this work we use $E_{max,\rm p} = 500$ EeV for protons and $E_{max,\rm Fe} = 156$ EeV for iron primaries. One should note that these choices are arbitrary.

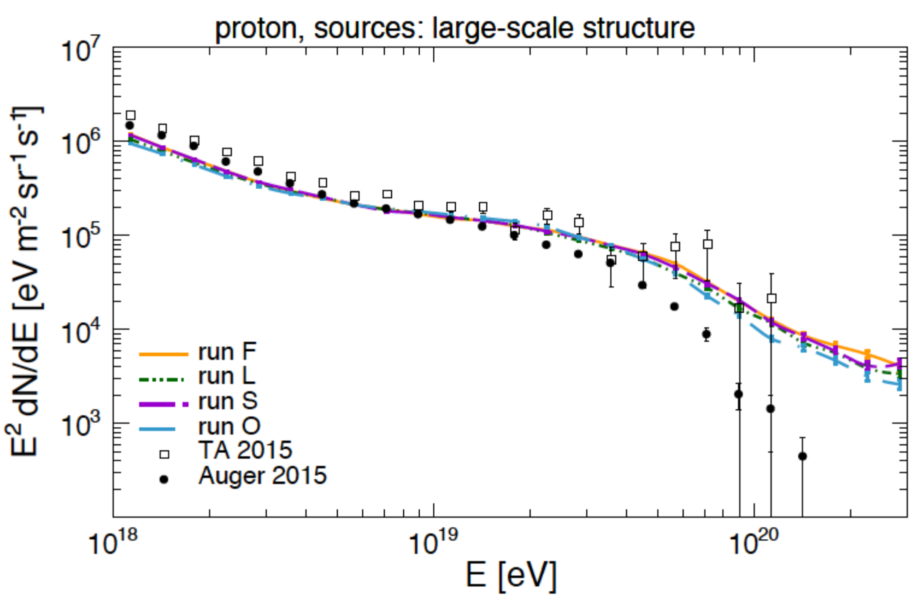

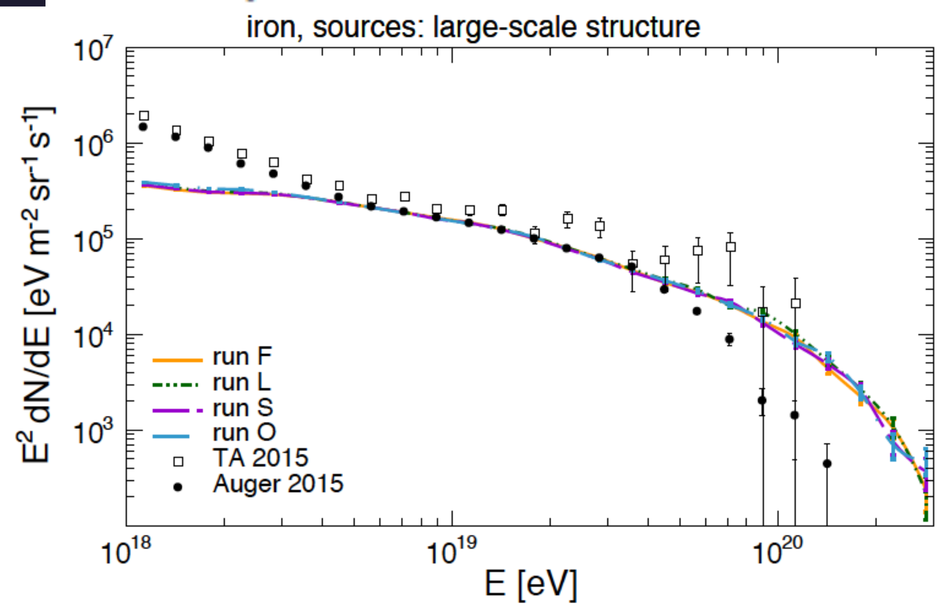

nucleus	E [EeV]	D [Mpc]	sources	run F	run L	run S	run O
p	10	0-10	uni	$21.4° \pm 11.5°$	$31.7° \pm 19.6°$	$30.5° \pm 16.5°$	$67.6° \pm 24.6°$
p	10	0-10	lss	$41.3° \pm 16.2°$	$60.0° \pm 21.1°$	$42.9° \pm 17.4°$	$81.6° \pm 21.0°$
p	60	0-5	uni	$1.5° \pm 1.1°$	$1.7° \pm 1.5°$	$2.3° \pm 1.3°$	$4.0° \pm 2.8°$
p	60	0-5	lss	$4.3° \pm 2.0°$	$8.8° \pm 6.1°$	$4.7° \pm 2.4°$	$27.1° \pm 16.0°$
p	60	0-10	uni	$2.5° \pm 1.4°$	$3.0° \pm 3.2°$	$3.1° \pm 1.6°$	$6.9° \pm 4.0°$
p	60	0-10	lss	$4.9° \pm 2.4°$	$9.8° \pm 6.3°$	$5.5° \pm 2.7°$	$27.3° \pm 15.6°$
p	60	0-10	uni	$2.5° \pm 1.4°$	$3.0° \pm 3.2°$	$3.1° \pm 1.6°$	$6.9° \pm 4.0°$
p	60	0-10	lss	$4.9° \pm 2.4°$	$9.8° \pm 6.3°$	$5.5° \pm 2.7°$	$27.3° \pm 15.6°$
p	60	10-20	uni	$5.1° \pm 2.3°$	$7.4° \pm 3.1°$	$6.4° \pm 3.3°$	$21.7° \pm 13.0°$
p	60	10-20	lss	$7.4° \pm 2.8°$	$13.8° \pm 7.9°$	$7.2° \pm 2.8°$	$35.7° \pm 15.3°$
p	60	20-30	uni	$6.8° \pm 2.2°$	$10.8° \pm 4.2°$	$8.5° \pm 3.7°$	$34.7° \pm 16.6°$
p	60	20-30	lss	$8.4° \pm 3.3°$	$15.3° \pm 7.0°$	$9.0° \pm 3.5°$	$44.0° \pm 16.8°$
p	100	0-5	uni	$0.9° \pm 0.5°$	$1.0° \pm 1.1°$	$1.3° \pm 0.8°$	$2.1° \pm 2.7°$
p	100	0-5	lss	$2.3° \pm 1.1°$	$5.0° \pm 3.2°$	$2.7° \pm 1.4°$	$14.7° \pm 11.5°$
p	100	0-10	uni	$1.3° \pm 0.8°$	$1.8° \pm 1.5°$	$2.0° \pm 1.3°$	$3.9° \pm 4.8°$
p	100	0-10	lss	$2.8° \pm 1.3°$	$5.6° \pm 3.4°$	$2.9° \pm 1.5°$	$16.0° \pm 10.9°$
p	100	10-20	uni	$2.9° \pm 1.2°$	$4.5° \pm 2.0°$	$3.8° \pm 1.7°$	$10.6° \pm 7.5°$
p	100	10-20	lss	$4.1° \pm 1.7°$	$8.5° \pm 4.9°$	$4.3° \pm 1.8°$	$23.9° \pm 12.3°$
p	100	20-30	uni	$4.0° \pm 1.4°$	$6.0° \pm 3.0°$	$5.2° \pm 2.1°$	$19.3° \pm 11.3°$
p	100	20-30	lss	$4.8° \pm 1.7°$	$8.9° \pm 3.2°$	$5.0° \pm 1.6°$	$26.6° \pm 12.4°$
Fe	60	0-5	uni	$44.3° \pm 20.9°$	$43.6° \pm 20.0°$	$60.9° \pm 22.5°$	$64.6° \pm 23.1°$
Fe	60	0-5	lss	$76.6° \pm 23.5°$	$82.0° \pm 20.6°$	$70.0° \pm 21.8°$	$77.0° \pm 19.5°$
Fe	60	0-10	uni	$58.4° \pm 22.4°$	$67.3° \pm 23.3°$	$73.2° \pm 21.7°$	$77.6° \pm 22.6°$
Fe	60	0-10	lss	$78.6° \pm 22.4°$	$83.0° \pm 20.2°$	$78.9° \pm 21.5°$	$81.2° \pm 19.4°$
Fe	60	20-30	uni	$84.4° \pm 18.6°$	$87.7° \pm 19.5°$	$84.3° \pm 19.5°$	$90.2° \pm 20.3°$
Fe	60	20-30	lss	$84.0° \pm 19.7°$	$89.7° \pm 21.2°$	$90.7° \pm 19.6°$	$89.9° \pm 19.0°$
Fe	100	0-5	uni	$16.4° \pm 9.5°$	$32.0° \pm 21.2°$	$45.9° \pm 23.5°$	$51.8° \pm 23.7°$
Fe	100	0-5	lss	$56.0° \pm 20.6°$	$68.1° \pm 21.1°$	$60.9° \pm 21.5°$	$75.5° \pm 24.1°$
Fe	100	0-10	uni	$36.3° \pm 19.8°$	$48.2° \pm 23.1°$	$54.4° \pm 22.9°$	$69.7° \pm 24.0°$
Fe	100	0-10	lss	$64.0° \pm 20.3°$	$71.2° \pm 21.4°$	$64.8° \pm 21.6°$	$73.6° \pm 22.1°$
Fe	100	20-30	uni	$72.5° \pm 17.5°$	$84.3° \pm 20.0°$	$80.3° \pm 23.4°$	$77.4° \pm 17.1°$
Fe	100	20-30	lss	$92.4° \pm 17.7°$	$76.5° \pm 19.0°$	$75.7° \pm 16.5°$	$78.6° \pm 19.3°$

Alves Batista et al., in preparation

Full spectrum & composition

SNRs

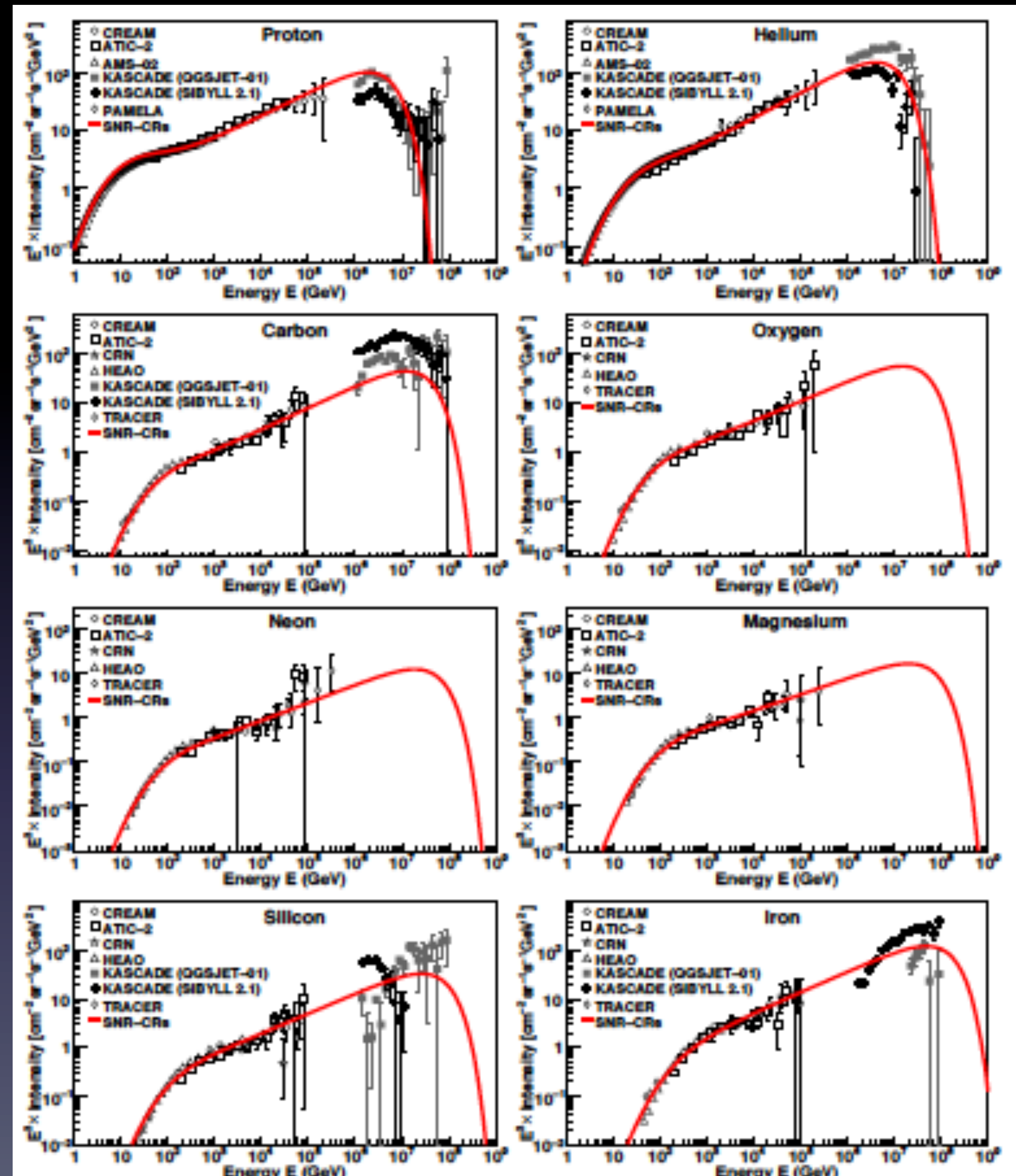

Full spectrum & composition

SNRs combined

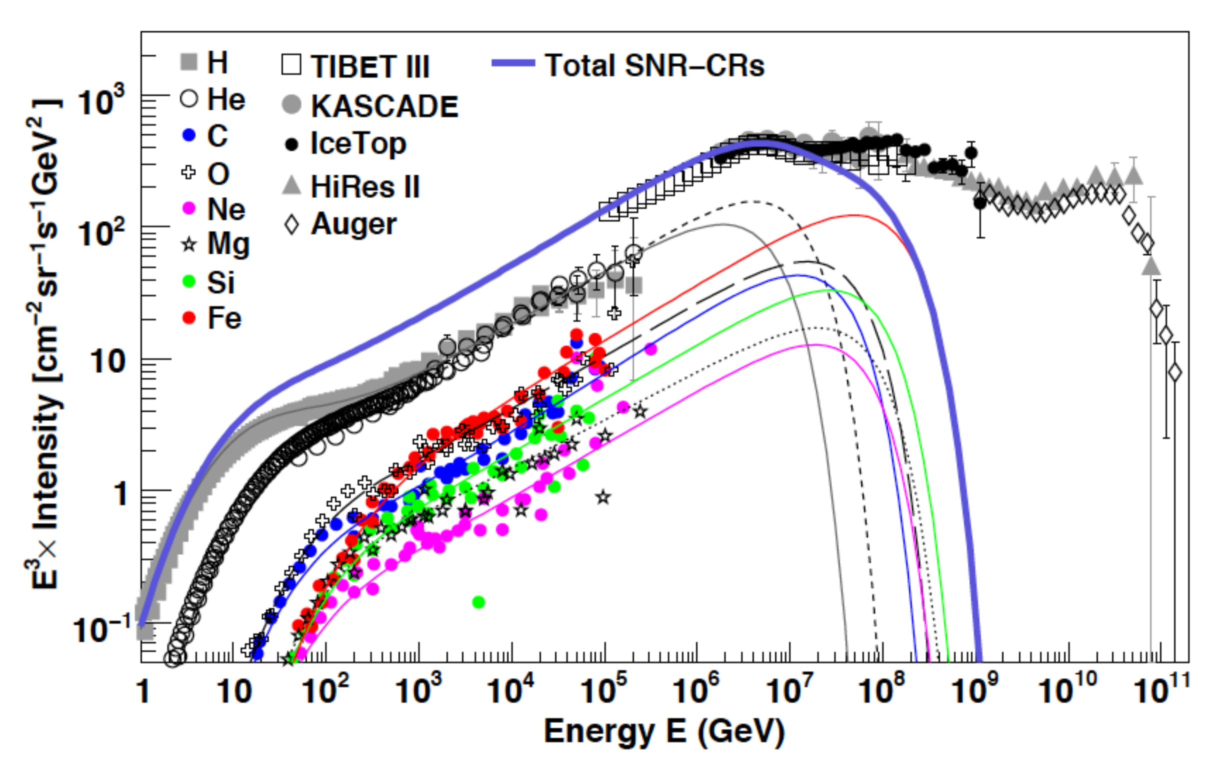

Full spectrum & composition

- 2^{nd} Galactic component
- Reacceleration by Galactic wind termination shocks
- Wolf-Rayet star explosions

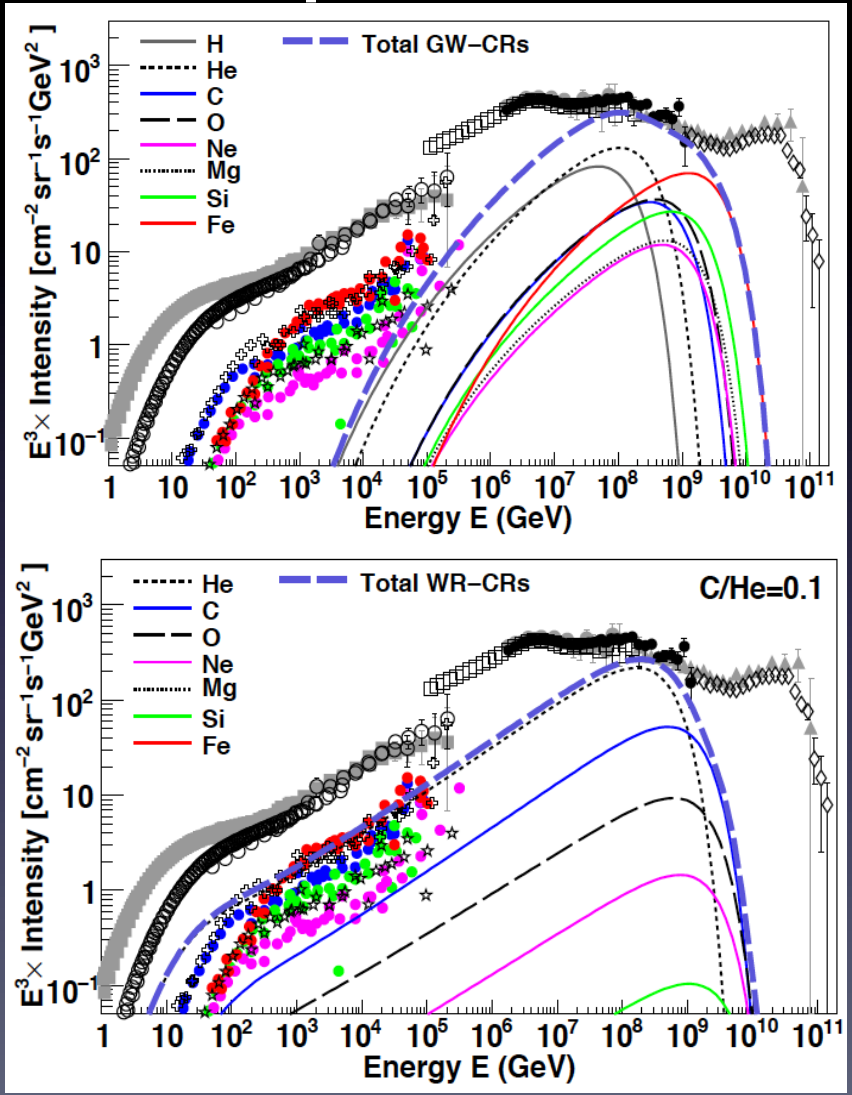

Full spectrum & composition

- Combined
- SNRs + WR-CRs + 3 different extragalactic models